

Chapter 3

Chaos Theory for Evolutionary Algorithms Researchers

Sergej Celikovsky and Ivan Zelinka

Abstract. This chapter deals with chaotic systems. Based on the characterization of deterministic chaos, universal features of that kind of behavior are explained. It is shown that despite the deterministic nature of chaos, long term behavior is unpredictable. This is called sensitivity to initial conditions. We further give a concept of quantifying chaotic dynamics: the Lyapunov exponent. Moreover, we explain how chaos can originate from order by period doubling, intermittence, chaotic transients and crises. In the second part of the chapter we discuss different examples of systems showing chaos, for instance mechanical, electronic, biological, meteorological, algorithmical and astronomical systems.

3.1 Introduction

The discovery of the phenomenon of deterministic chaos brought about the need to verify manifestations of this phenomenon also in experimental data. Deterministically chaotic systems are necessarily nonlinear, and conventional statistical procedures, which are mostly linear, are insufficient for their analysis. If the output of a deterministically chaotic system is subjected to linear methods, such signal will appear as the result of a random process. Examples include Fourier spectral analysis, which will disclose nonzero amplitudes at all frequencies in a chaotic system,

Sergej Celikovsky

Institute of Information Theory and Automation,
Academy of Sciences of the Czech Republic,
Faculty of Electrical Engineering, Czech Technical University in Prague
e-mail: celikovs@utia.cas.cz

Ivan Zelinka

Tomas Bata University in Zlin, Faculty of Applied Informatics, Nad Stranemi 4511,
Zlin 76001, Czech Republic
and
VSB-TUO, Faculty of Electrical Engineering and Computer Science, 17. listopadu 15,
708 33 Ostrava-Poruba, Czech Republic
e-mail: zelinka@fai.utb.cz

and so chaos can be easily mistaken for random noise. Apart from the (now mature) signal analysis in both the time and frequency domains, methods operating in the phase space are gaining in importance. Within such methods, the trajectory of a dynamic system in the phase space is first reconstructed from the (usually scalar) time series, and the chaos descriptors are subsequently estimated or modelling is applied. This is a quite recent field of research, just going back to the discovery of the immersion theorem [19], [26] in the early 1980s. Despite lack of rigorous mathematical explanation of some issues, well interpretable results can be obtained with some caution. This is so, in particular, for low-dimensional systems, for the analysis of which such procedures have been primarily developed. Nevertheless, some rather naive applications and interpretations of results were attempted in the past. Examples of such simplified interpretations which contradict physical intuition have been cited by Drazin and King [11]. According to those authors, the early successes of nonlinear analysis of time series raised hopes that the day will come when we will be able, from periodical air temperature measurements behind the window, to identify the dynamics of the whole atmosphere, based on which the future climatic situation should be predictable.

One of the goals of this chapter is to explain why such a mechanistic interpretation of determinism is not correct. The main reason for that naive idea to fail is exactly the existence of the deterministic chaos.

This chapter discusses the most common topics of chaos theory, especially from the practical application aspects point of view. Common approaches to the reconstruction of the system trajectory in the phase space are summarized and procedures are outlined for estimating the correlation dimension, entropy and the largest Lyapunov exponent. Thereby, it a priori assumed that the sources of the time series examined are nonlinear chaotic systems. This is why, for example, nonlinearity tests are not described here. For the same reason, as well as due to the limited extent of this book some important components of nonlinear modelling of time series, such as nonlinear methods for noise prediction and reduction, are omitted. The interested reader may find more detailed information on that topic in monographs [2], [17], [10], [12].

3.2 Characterization of Deterministic Chaos

When hearing the word “chaos”, people who are not experts in this field may imagine a process which is of a purely random nature and lacks any internal rules. Just a few people realize that “being chaotic” actually means complying well defined and strictly deterministic rules”. As indicated in the historical outline, chaos is a discipline which obtained its name only in the 20th century but whose roots date back to the 18th and 19th centuries, associated with the finding that even simple problems may generate very complex and unpredictable solutions. For historical reasons, Hamiltonian systems were the first systems to be studied, represented then by celestial mechanics problems. Many rules valid for a wide class of Hamiltonian systems generating chaotic behavior were discovered. Later on, these rules were

extended to apply to some dissipative chaotic systems as well. Although it deals basically with dissipative systems, this publication will include a short excursion to other chaos generating systems as well.

3.2.1 Roots of Deterministic Chaos

The term “chaos” covers a rather broad class of phenomena whose behavior may seem erratic and unpredictable at the first glance. Often, this term is used to denote phenomena which are of a purely stochastic nature, such as the motion of molecules in a vessel with gas etc. This publication focusses on the deterministic chaos, a phenomenon which - as its name suggests - is not based on the presence of a random, stochastic effects. On the contrary, it is based on the absence of such effects what may seem surprising at the first glance. Broadly used, the term “chaos” can denote anything that cannot be predicted deterministically (e.g. motion of an individual molecule, numbers in a lottery, ...). If, however, the word “chaotic” is combined with an attribute such as “stochastic” or “deterministic”, then a specific type of chaotic phenomena is involved, having their specific laws, mathematical apparatus and a physical origin. Stochastic system (not stochastic chaos) is the appropriate term for a system such as plasma, gas, liquid, which should be studied by using a suitable apparatus of plasma physics, statistical mechanics or hydrodynamics. On the contrary, if a double pendulum, billiard or the similar objects are the subject of examination, a mathematical apparatus which is based on classical mathematics and does not exhibit “stigmata” of statistics is employed. The mathematical apparatus for the description and study of the systems was not chosen at random; in fact, it is related with the physical nature of the system being studied. Considering the class of systems of deterministic chaos as mentioned above, signs of chaotic behavior are usually conditional on the presence of nonlinearities, either in the system itself (i.e. the system is a nonlinear system) or in links between linear systems [14]. Usually, such nonlinearities are only visible after making up a mathematical model of the system or after analysis of observed data. Simple systems exhibiting deterministic chaos include, for instance, double pendulum, magnetic pendulum, electronic circuit or a set of bars (Fig. 3.1) over which balls are poured from “the same” starting position. Since the individual examples are discussed in this monograph below, the focus will now be on the last-mentioned example. The example involves a very simple mechanical system which is an analogy of the well-known billiard problem. As Fig. 3.1 demonstrates, the entire mechanical system consists of a set of bars which are held by a vertical board and over which balls are poured from “the same” position. Although released from the same position, each ball follows a different pathway. This is so because the starting conditions are not absolutely identical; instead, they differ very slightly, even negligibly at first glance. It is those differences that are responsible for the fact that the trajectories differ appreciably. In other words, the system is sensitive to the initial conditions.

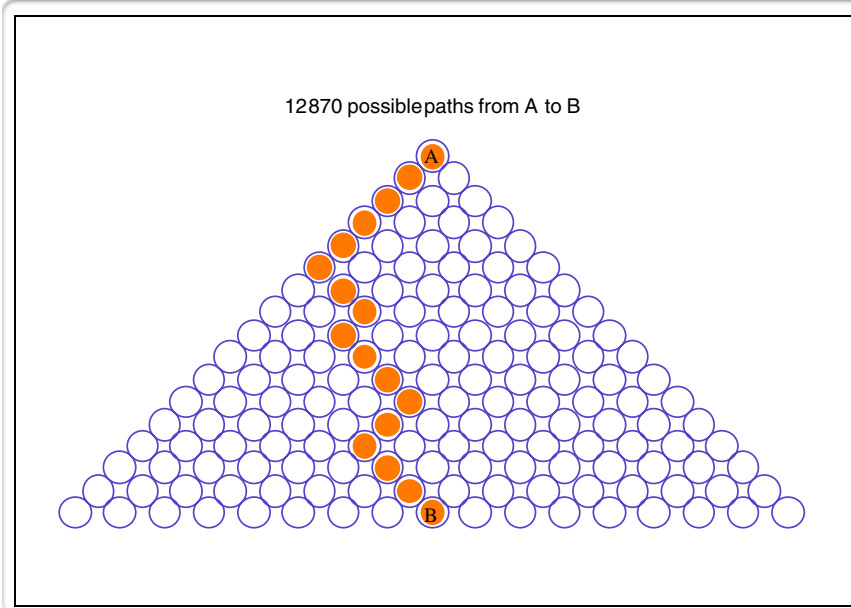


Fig. 3.1 One of the possible realizations of the billiard problem

This sensitivity to the initial conditions is a phenomenon which is related to the billiard problem. Basically, the cause is in the fact that the mechanical objects hitting each other do not possess ideally smooth surfaces. Due to this, even the slightest differences in the initial conditions are “amplified”, ultimately giving rise to different trajectories. The nonlinear model shown in Fig. 3.1 can serve as a next model of the billiard problem. Two types of trajectory are involved: periodic (Fig. 3.2) and chaotic (Fig. 3.3). The axes of incidence and recoil of the hypothetical ball are shown. Fig. 3.4 demonstrates the creation of chaos. The ball was started from a nearly identical position with a difference of 1×10^{-12} in this simulation. Different trajectories (red and green) can be discriminated after 25 iterations.

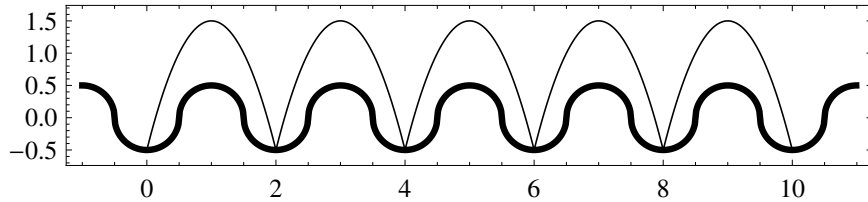
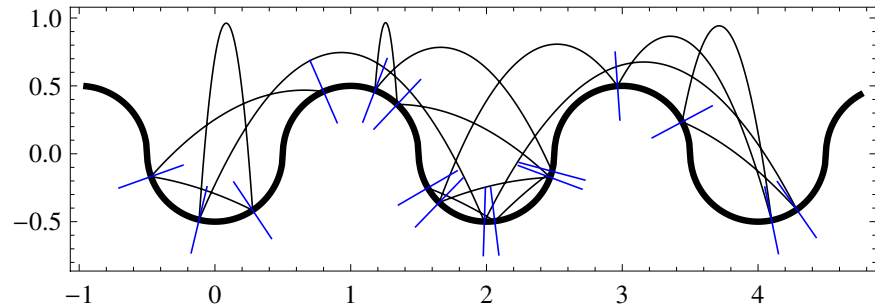
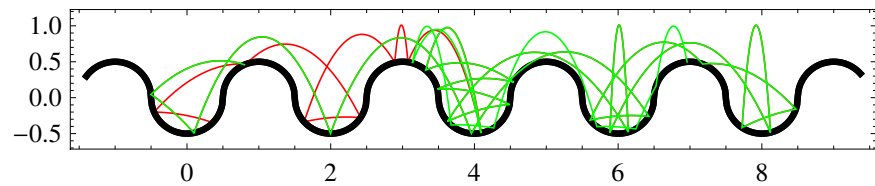
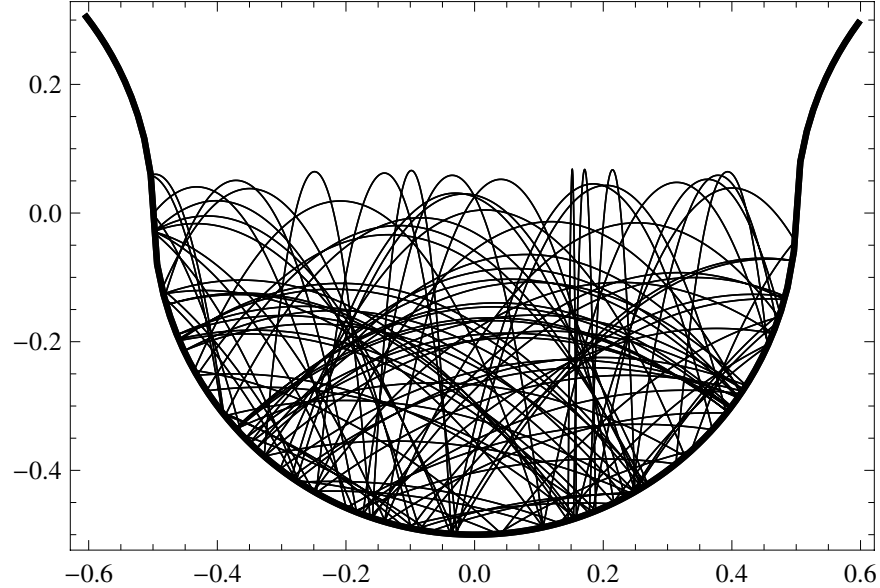


Fig. 3.2 Deterministic behavior at billiard

**Fig. 3.3** Chaotic behavior at billiard**Fig. 3.4** Chaotic behavior at billiard, difference in the initial conditions was 1×10^{-12} . After 25 iterations trajectories has diverged.**Fig. 3.5** Chaotic behavior at simple billiard, no periodical behavior is visible. 500 iterations from 10 000 is depicted at this picture.

Chaos can be visualized not only in the manner shown in the figures but also by means of interdependences of quantities of state. A trajectory having a total length of 10 000 iterations (Fig. 3.5, only 500 iterations are shown) was generated for this purpose. A rather wealthy set of types of behavior can be encountered in the real world. One of the possible categorizations is included in Table 3.3. The table encompasses both purely stochastic types of behavior (coin toss, thermal noise, ...) and deterministic types of behavior (celestial mechanics), including chaos (intermittence, chaotic attractors, ...).

Table 3.1 Possible types of behavior of dynamic systems [14]

Behavior	Example
Predictable	Planets
Unpredictable	Coin toss
Chaotic transitions	Billiard problem
Intermittence	Logistic equation (for $A = 3.8284$)
Narrow-band chaos	Rössler attractor
Low-dimensional broadband chaos	Lorenz attractor
High-dimensional broadband chaos	Neuron networks
Correlated (colored) noise	Random walk
Pseudorandomness	Computer-generated randomness
Randomness	Thermal noise, radioactivity
Combination of the above types of behavior	Real data

3.2.1.1 Hamiltonian Systems

The study of Hamiltonian systems has its roots in the 19th century when it was introduced by Irish mathematician William Hamilton. For mechanical systems, a typical feature of Hamiltonian systems is that no dissipation of energy occurs in them, so that mechanical Hamiltonian system is also the so-called conservative one. In general dynamical system theory the term “conservative” means that certain scalar function, having typical properties of energy, is preserved along system trajectories. The creation of chaos theory for Hamiltonian systems was contributed to by scientists such as Boltzman (who laid the foundations of ergodic theory and discovered the contradiction between the reversibility of a system and irreversibility of its behavior) and Poincare. Assets of Hamiltonian systems included their amenability to solution without the deployment of computer techniques, something we can hardly imagine today. The mathematical apparatus and thus also the philosophy of Hamiltonian systems find application in many areas of physics, such as plasma physics, quantum mechanics and others.

3.2.1.2 Dissipative Systems

Dissipative dynamic systems are systems where energy escapes into the surroundings and state space volume is reduced. Typical examples include weight on spring

(dissipation being caused by friction between the body and air and energy losses inside the material), motion on a wheel, electronic resonance circuits. Since the topics of dissipative dynamic systems is the subject of a whole monograph, demonstration of a concrete real system, see the classical oscillating cell, will be given here. This well-known classical example of a dynamic system is defined by the Lorenz system (3.2).

3.3 Universal Features of Chaos

Deterministic chaos possesses many features that are common to chaotic behavior irrespective of the physical system which is the cause of this behavior. This common nature is expressed by the term universality so as to stress the universal nature of the phenomena. The quantity and properties of the features as well as the complexity of links between them are so extensive that they could make up a topic for a separate publication, such as [9]. It is not the aim of this part of the publication to make a detailed analysis - this would be like carrying coals to Newcastle; instead, only the best-known features, to be used in the subsequent sections of this book, will be highlighted. These include, in particular, Feigenbaum's constants α and δ , the U -sequence, Lyapunov exponents, self-similarity and processes by which a system usually passes from deterministic behavior to chaotic behavior: intermittence, period doubling, metastable chaos and crises. Another property which is, curiously, not included in the pantheon of universalities will be mentioned at the beginning: the deterministic nature and non-predictability of deterministic chaos.

3.3.1 Determinism and Unpredictability of the Behavior of Deterministic Chaos – Sensitivity to Initial Conditions

The deterministic structure of systems which generate chaos and their unpredictability constitute another typical feature of the universal properties of deterministic chaos. It is actually irrelevant what type the chaotic system is (chemical, biological, electronic, economic, ...): it holds invariably that their mathematical models are fully deterministic (there is no room for randomness as such in them) and they are long-term unpredictable in their behaviour. The Rössler (3.1) and Lorenz (3.2) attractors are the typical examples:

$$\begin{aligned}\dot{x}_1(t) &= -x_2(t) - x_3(t) \\ \dot{x}_2(t) &= -x_1(t) - \frac{x_2(t)}{5} \\ \dot{x}_3(t) &= (x_1(t) - 5.7)x_3(t) + 0.2\end{aligned}\tag{3.1}$$

$$\begin{aligned}\dot{x}_1(t) &= -a(x_1(t) - x_2(t)) \\ \dot{x}_2(t) &= -x_1(t)x_3(t) + bx_1(t) + x_3(t) \\ \dot{x}_3(t) &= x_1(t)x_2(t) - x_3(t).\end{aligned}\tag{3.2}$$

It is clear from the structure of the equations that no mathematical term expressing randomness is present. That apparent randomness that can be seen in deterministic chaos at first glance is not purely fortuitous; in fact, it is related to the sensitivity to initial conditions. This sensitivity can be demonstrated well on the example of a smooth hill from whose top a ball is let run down. The ball will take a different trajectory in each experiment, which is due to two factors: the first is the non-ideality of the hill surface, the other, impossibility of setting the starting position absolutely identically when repeating the experiment. The inaccuracies are due to the ubiquitous error of measurement (in manufacturing the hill, in setting the position, in manufacturing the ball, ...), and even if all the errors could be eliminated, the uncertainty of the quantum world (i.e. Heisenberg uncertainty principle) would ultimately take effect and act in the macro-world as well (which it actually does). Hence, fluctuations cannot be avoided, and so “declaring total war” on fluctuations is a waste of time and akin to Don Quixote’s tilting at windmills. A normal PC with appropriate software will do for experiments with sensitivity to initial conditions. Fig. 3.6 demonstrates sensitivity to initial conditions for the Lorenz attractor. Two time developments of the variable of state x (Fig. 3.6) are shown for a difference between the initial conditions $\Delta y(0) = 0.001$, which appears as a negligible error at first glance. However, in a time as short as 24 seconds the two state trajectories diverge, as emphasized by the grey area between them. (Fig. 3.7) shows the same for $\Delta y(0) = 10^{-9}$. Sensitivity to initial conditions is thus one of the characteristic features of deterministic chaos and can be used as an indicator when classifying a dynamic system.

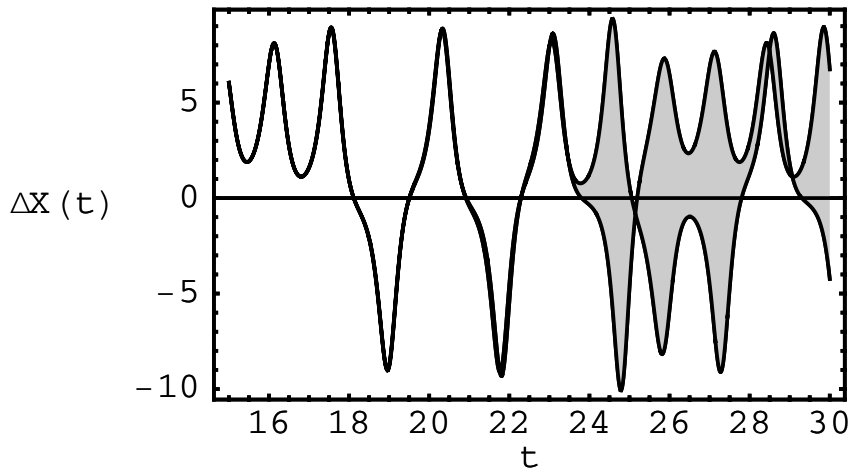


Fig. 3.6 Sensitivity of the variable x of the Lorenz attractor for $\delta y(0) = 0.001$

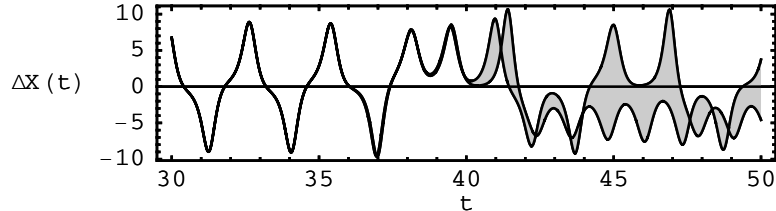


Fig. 3.7 Sensitivity of the variable x of the Lorenz attractor for $\delta y(0) = 10^{-9}$

3.3.2 Lyapunov Exponents

Lyapunov exponents are another member of the family of universal features of deterministic chaos. They are numbers which basically express the divergence (or also convergence) of the state trajectories of a dynamic system. The exponents can be calculated relatively simply, both for discrete-time systems and for continuous-time systems. As will be explained later, Lyapunov exponents are closely related to the structure of the state space, which (in dynamic systems theory) is represented by an array of arrows determining the time development of the system at each point of the space. The development of the system in this space is then represented by a (usually) continuous curve [24].

The effect of Lyapunov exponents on the behavior of the dynamic system is apparent from Fig. 3.8 and 3.9. Figure 3.8 shows the state space of a simple dynamic system along with two different time developments starting from two different initial conditions, which only differ by $\Delta x = 0.01$ in the x -axis. The behavior in the

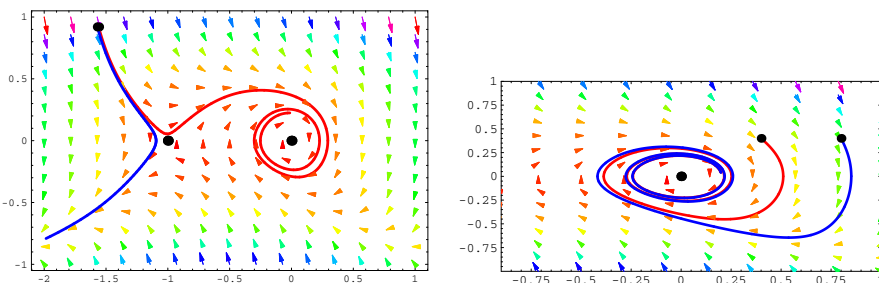


Fig. 3.8 State space trajectory for a dynamic system with 2 singular points s_1 and s_2 . On the position $s_1 = \{0,0\}$ is repeller and at the position $s_2 = \{-1,0\}$ saddle. Start points of both trajectories diverge despite fact that this coordinates ($x_1 = \{-1.56, 0.92\}$ and $x_2 = \{-1.57, 0.92\}$) are very close.

Fig. 3.9 Different behavior can be observed when both trajectories will start in different part of state space. Despite its bigger difference in starting position ($x_1 = \{0.4, 0.4\}$ and $x_2 = \{0.8, 0.4\}$) trajectories merge together after certain time.

two cases is entirely different. Figure 3.9 shows different behavior. Hence, the behavior of a dynamical system is determined by its physical structure, which in the mathematical description is represented by the state space whose quantifiers can be Lyapunov exponents. If one is to follow colored arrows in Fig. 3.8, it can be noticed that they are separating with increasing time. On the other hand in Fig. 3.9 they after certain time occupy the same set of points in the state space, in this case called limit cycle. This observation can be described in a mathematical way by the Lyapunov exponent λ , see eq. 3.3. The structure of the exponents can help assess whether chaotic behavior is present in the system or not.

Consider a situation where at time $t_0 = 0$, a hypersphere whose radius is $l(0)$ exists in the m -dimensional phase space. Let different points of the hypersphere surface represent different initial conditions of the dynamical system. Hence, starting from each point of the hypothetical hypersphere, construct a trajectory through the phase space. After time t the hypersphere transforms into a new object. In the general case, this object can have a very complicated shape, especially if the dynamics are chaotic. However, if we restrict ourselves to very short time segments $[0, t]$ and if the initial radius $l(0)$ is also very small, one can assume for simplicity that the initial hypersphere is transformed, in the ideal case, into a hyper ellipsoid. Denote $l_i(t)$ the length of the semi-major axes of the ellipsoid formed at time t . The i_{th} Lyapunov exponent

$$\lambda_i = \lim_{t \rightarrow \infty} \frac{1}{t} \ln \frac{l_i(t)}{l(0)} \quad (3.3)$$

is a measure of the extension or contraction of the i_{th} semi-major axis of the ellipsoid. For graphic reasons, Lyapunov exponents are arranged by magnitude, i.e. $\lambda_1 \geq \lambda_2 \geq \dots \geq \lambda_m$, where m is the dimension of the phase space; this is referred to as the Lyapunov exponents spectrum. For a chaotic trajectory, at least one Lyapunov exponent must be positive, although, in addition, the existence of any asymptotic periodicity must be ruled out to confirm the chaotic nature - see, e.g., [3]. In other words, the possibility that the trajectory converges to some periodic orbit with $t \rightarrow \infty$ must be eliminated. But it is just this requirement that can pose a problem in practice if the dynamical system is investigated during a finite time interval only. Chaotic systems with more than one Lyapunov exponent are referred to as hyperchaotic [22].

Owing to the limit $t \rightarrow \infty$, Lyapunov exponents introduced by eq. (3.3) are global quantities describing the system dynamics on average. Nevertheless, relating Lyapunov exponents to a certain part of the trajectory for a relatively short time segment t also proved to be useful. This leads to the concept of a local Lyapunov exponent [2], [30]. It will be clear from the above text that Lyapunov exponents represent the rate of divergence (or convergence) of near trajectories in the phase space, thus providing a measure of predictability. Hence, this warrants the question as to how Lyapunov exponents relate to Kolmogorov entropy. The relation can be expressed as follows [22]:

$$K \leq \sum_{i, \lambda_i > 0} \lambda_i \quad (3.4)$$

where equality occurs for the Sinai-Ruelle-Bowen measure, i.e. the measure which is smooth along an unstable manifold. Equality between Kolmogorov entropy and the sum of positive Lyapunov exponents is referred to as Pesin identity [23]. Now, examine the relationship between Lyapunov exponents and fractal dimension. If Lyapunov exponents are negative for all i 's ($\lambda_i < 0$), each attractor of such a system must be a fixed point and thus have a zero dimension. And on the contrary, if $\lambda_i > 0$ for all i 's, the trajectories in the phase space go apart constantly in all directions and the dimension converges to that of the phase space [30]. Hence, one will ask what the relation between Lyapunov exponents and the fractal dimension is. Using the spectrum of Lyapunov exponents $\lambda_1 \geq \lambda_2 \geq \dots \geq \lambda_m$, J. L. Kaplan and J. A. Yorke introduced the concept of Lyapunov dimension, sometimes referred to as the Kaplan-York dimension. If k is the largest non-negative integer for which

$$\sum_{i=1}^k \lambda_i \geq 0 \quad (3.5)$$

then Lyapunov dimension is defined as follows [15]:

$$d_L = \begin{cases} 0 & \text{if no such } k \text{ exists} \\ k + \frac{\sum_{i=1}^k \lambda_i}{|\lambda_{k+1}|} & \text{if } k < m \\ m & \text{if } k = m \end{cases} \quad (3.6)$$

In this definition, m has the meaning of the phase space dimension. General equality between Lyapunov dimension and some of the other fractal dimensions has not been proved so far. Many numerical experiments lead to the approximate equality $d_L \approx d_1$, d_L is given by eq. (3.6), d_1 is so called informational dimension, see eq. (3.7)

$$d_1 = \lim_{r \rightarrow 0} \frac{-S(r)}{\log_2 r} = \lim_{r \rightarrow 0} \frac{\sum p_i \log_2 p_i}{\log_2 r}, \quad (3.7)$$

equality between these two dimensions being found for two dimensional mappings [18]. It is generally believed that Lyapunov dimension and information dimension are equal for "typical" attractors [20], [15]. A general rule holds [8] that Lyapunov dimension is the upper limit of Hausdorff dimension. The fact that knowledge of Lyapunov exponents gives us an idea of fractal dimension can be used when testing procedures for estimating attractor dimension from time series. With the knowledge of the system control equations in the form of difference equations or ordinary differential equations the calculation of Lyapunov exponents is "merely" a technical - although not necessarily easy - task. Having calculated Lyapunov dimension from the Lyapunov exponents spectrum and adopting the hypothesis of its closeness to other fractal dimensions, the value of the dimension so obtained can be compared with the estimate based on the time series generated by the system control equations and, tentatively at least, assess the adequacy of some algorithms for nonlinear analysis of time series. The same approach can be used to examine procedures for the

calculation of Kolmogorov entropy from experimental data, assuming validity of Pesinov identity. Now, pay some attention to the time of predictability of the system behavior, as mentioned earlier. Imagine a dynamic system with one positive Lyapunov exponent λ . The initial state of the system is known with accuracy ε . After time T , the position of the system in the phase space is known with accuracy L . Taking into the account eq. (3.3) we have [5]

$$\lambda \approx \frac{1}{T} \ln \frac{L}{\varepsilon}, \quad (3.8)$$

which implies that

$$T \approx \frac{1}{\lambda} \ln \frac{L}{\varepsilon} \approx \frac{1}{K} \ln \frac{L}{\varepsilon}, \quad (3.9)$$

where K is Kolmogorov entropy. Time T expresses the time in which inaccuracy ε in the determination of the initial conditions increases exponentially. This time is usually referred to as the system behavior predictability time. However, the relation above indicates that this time is not only dependent on the dynamics of the system (Lyapunov exponents); in fact, the magnitude of the initial error also plays a role: time T increases logarithmically with increasing initial accuracy. Time T can be only crudely identified with the predictability time and only within the context of the accuracy considered, which should be chosen reasonably. If you forecast, for instance, that the next winter will be colder than the past summer, you will probably be right but such prediction is actually useless for the vast majority of purposes.

3.3.3 The U-Sequence

The universal sequence, or the *U*-sequence, is another universal feature of deterministic chaos. The *U*-sequence is frequently demonstrated on iterated maps, whose typical representative is the well-known logistic equation. The *U*-sequence can be observed in the behavior of a number of dynamic systems whose mathematical model contains unimodal mapping (with one extremum). The logistic equation, formulated as eq. (3.11), is a typical example. The term unimodal mapping denotes the dependence of a next value on the preceding values when the control parameter is varied. For instance, if eq. (3.11) is considered and the control parameter A is varied within the interval of $[0, 4]$, the functional dependence shown in Fig. 3.10 emerges. The value at which this dependence attains its maximum is usually referred to as the critical point [16]. This value is 0.5 in Fig. 3.10, as indicated by a vertical ordinate. When the initial conditions are set, the development of the system is shown graphically as a sequence of points (Fig. 3.11) and 3.11 on the unimodal curve. The points of this sequence are assigned the letter L or R according to whether they lie to the left or to the right of the critical point.

U-sequences listed in Table 3.3 can be observed for the logistic equation. This and other sequences are also observable with other mathematical models of dynamic systems.

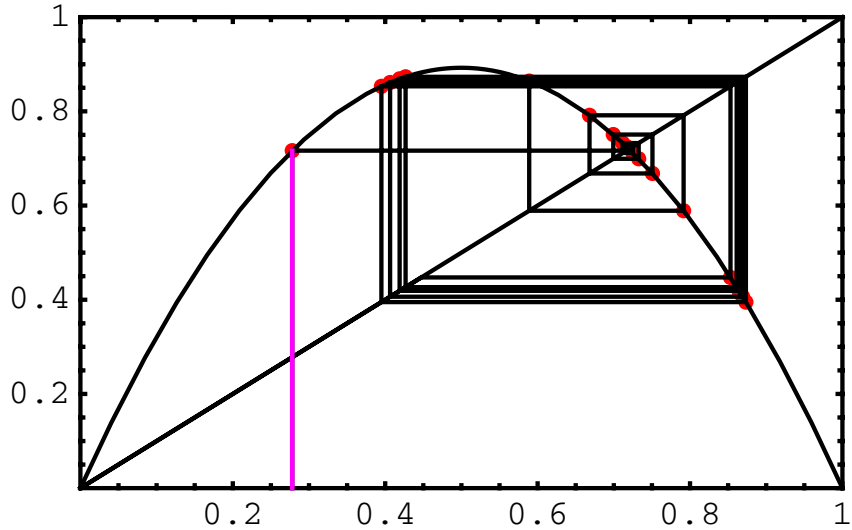


Fig. 3.10 Unimodal sequence of the logistic equation

Table 3.2 U-sequence according to [0]

Perioda	U-sequence	Parameter A value
2	R	3.2361
4	RLR	3.4986
6	RLRRR	3.6275
5	RLRR	3.7389
3	RL	3.8319
6	RLLRL	3.8446
5	RLLR	3.9057
6	RLLRR	3.9375
4	RLL	3.9603
6	RLLLRL	3.9778
5	RLLL	3.9903

A graphic presentation of such sequences is also possible in 2D graphs by assigning white color to the R-positions and black color to the L-positions. Therefore, one can easily see when U-sequences agree with one another. Figs 3.11 and 3.12 depict the *U*-sequences for the logistic equation and for the following equation

$$x_{n+1} = 1 - Cx_n^2 \quad (3.10)$$

called as the quadratic one. The sequences are the same for $A = 3.3$ in the former equation and $C = 1.1$ in the latter equation.

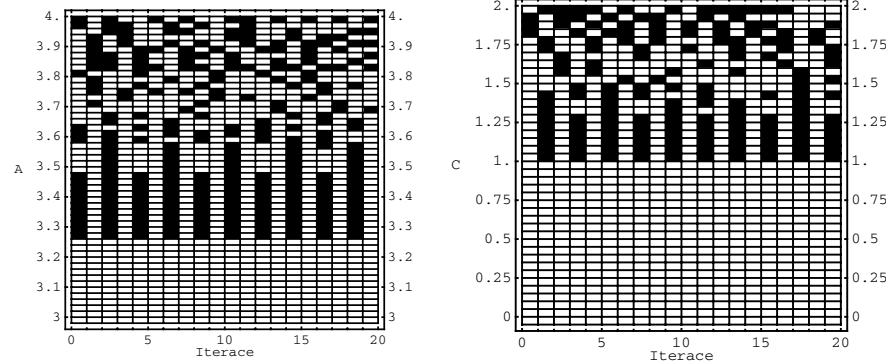


Fig. 3.11 Graphical representation of the U-sequence for the logistic equation with parameter A

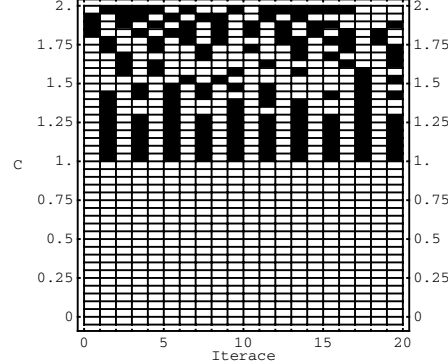


Fig. 3.12 Graphical representation of the U-sequence for the quadratic equation with parameter C

3.3.4 Intermittence, Period Doubling, Metastable Chaos and Crises

The emergence of chaos is not a phenomenon that can be described as a purely discrete event; instead, it has a “transient phase” during which the system behavior changes from predictable to chaotic, both by a deterministic pathway and by a random pathway. The two processes are often intertwined, representing thus a kind of “universal” pathway to chaos. Period doubling is a typical example of a deterministic transition [16]. This is a phenomenon where the period of the system behavior doubles and at some control parameter levels transforms into chaotic behavior. This is demonstrated for the logistic equation in Fig. 3.13 and 3.14, where the left part displays the period doubling mode and the right part displays intermittence. It is of interest to note that the geometric objects which are seen on the right in Fig. 3.14, having a triangular shape (iterations 30 - 40, 50 - 60), are known from stock exchange developments and are employed for near-future time series behavior estimates.

The emergence of intermittence [16] is associated with very fine changes in the control parameter, which can be due to noise or, for instance, to numerical instability. Due to such fine changes the system behavior changes dramatically, being transferred from one type of behavior to the other. The emergence of intermittence from the logistic equation is shown in Figs 3.15 and 3.16 by means of the WEB diagram [16], [6]. A web diagram, also sometimes called a cobweb plot, is a graph that can be used to visualize successive iterations of a function $x_{n+1} = f(x_n)$. The diagram is called WEB because its straight line segments “anchored” to the functions and can resemble a spider web - thus WEB diagram.

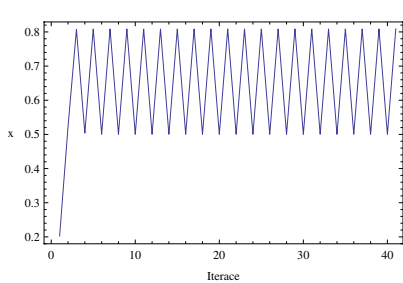


Fig. 3.13 Period doubling for the logistic equation...

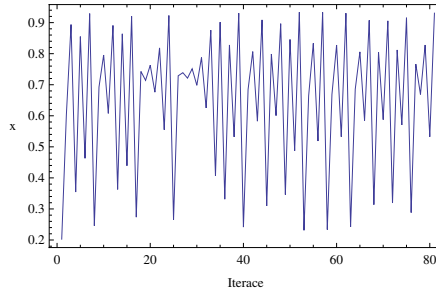


Fig. 3.14 ... and intermittence.

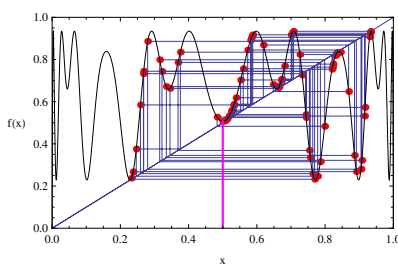


Fig. 3.15 WEB diagram of the logistic equation for $A = 3.7375$ and 70 iterations

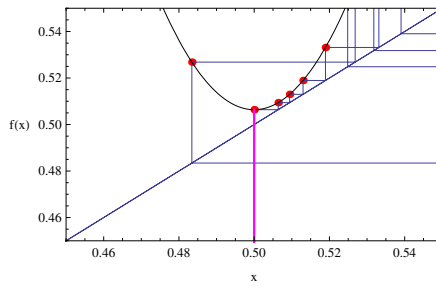


Fig. 3.16 WEB diagram (detail) of the logistic equation for $A = 3.7375$ and 70 iterations

In Fig. 3.16 a small change causes the behavior to “switch” to the chaotic mode whose overall appearance is shown in Fig. 3.15. If this change is due to a continuous change in the control parameter, a crisis (see later) can take place if promoted by the configuration of the system. This means that the entire chaotic attractor can vanish or be replaced by another attractor [16]. A little bit more detailed analysis of the various pathways leading to chaos will be presented later in this Chapter.

3.3.5 Feigenbaum Constants

As mentioned in the section highlighting the history of theories dealing with deterministic chaos, the theoretical physicist Mitchell Feigenbaum devised two constants which certainly belong to the set of universalities of deterministic chaos. Their nature and application can be best explained using examples which include graphical visualization of the development of a chaotic system, specifically bifurcation diagrams (Fig. 3.17).

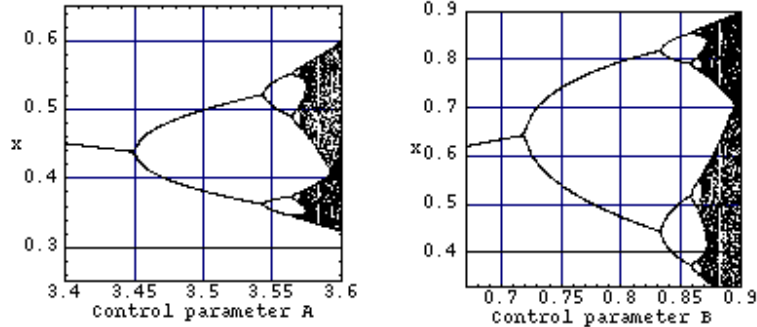


Fig. 3.17 Source of Feigenbaum's constants - self-similarity of bifurcation diagrams. Left: diagram for the logistic equation (3.11); right: section for the equation containing the trigonometric function, eq. (3.12).

The diagrams were generated by using (3.11) and (3.12):

$$x_{n+1} = Ax_n(1 - x_n) \quad (3.11)$$

$$x_{n+1} = B\sin(\pi x_n) \quad (3.12)$$

They differ in a comprehensive representation (Fig. 3.17) but a detailed view shows that different systems can produce virtually identical behavior: Two Feigenbaum's constants α and δ follow from Fig. 3.17. Basically, they are numbers (constants) representing geometric convergence of bifurcation diagrams. Both diagrams exhibit branch splitting which proceeds in a very similar manner, as regards both the x -axis and the y -axis. This can be seen in detail in Fig. 3.17.

Fig. 3.17 demonstrates that when the control parameter is changed, the system behavior changes so that the branches in the bifurcation diagram are divided into two additional branches each while a distance from the most recent division is progressively diminishing. If the branching is projected into the x -axis and the ordinates in which the branching has taken place are denoted sequentially, a sequence of numbers is obtained expressing the geometric convergence of the bifurcation diagram with respect to the x -axis. This set of numbers also expresses the second Feigenbaum's constant, δ , given by relations (3.13) and (3.14).

$$\delta_n = \frac{A_n - A_{n-1}}{A_{n+1} - A_n} \quad (3.13)$$

$$\delta = \lim_{n \rightarrow \infty} \delta_n = 4.66920161\dots \quad (3.14)$$

Constant δ is the limit of numbers which can be understood, with some exaggeration, as "local Feigenbaum's constants". The first Feigenbaum's constant is α (which also precedes δ in the Greek alphabet). This constant is derived by a similar procedure. The branching process is accompanied by changes in the distance

between the points of branching, denoted d_n . Once again, constant α is given by the limit of the ratio of the current distance to the previous distance. The mathematical formula is given by eq. (3.15). The limiting sequences leading to the above constants can be calculated even from simple mathematical models, such as the logistic equation.

$$\alpha = \lim_{n \rightarrow \infty} \frac{d_n}{d_{n+1}} = 2.5029\dots \quad (3.15)$$

Feigenbaum's constants are physical parameters which are common to a wide class of systems. From how the constants are derived (as also indicated in [16]) also follows how they can be used, specifically, how δ can be used to predict additional bifurcations in the system. Realizing that δ describes the measure of subsequent bifurcations, the prediction principle is quite clear. Starting from eq. (3.13) and (3.14) and rearranging, one arrives at eq. (3.16), which can be used to calculate the control parameter value at which the next bifurcation will take place.

$$A_{n+1} = \frac{A_n - A_{n-1}}{\delta} + A_n \quad (3.16)$$

In this manner the values can be obtained, or as shown by relations (3.17) and (3.18).

$$A_3 = \frac{A_2 - A_1}{\delta} + A_2 \quad (3.17)$$

$$A_4 = \frac{A_3 - A_2}{\delta} + A_3 \quad (3.18)$$

Hence, the result is fully determined by the two preceding bifurcations. Substitution of eq. (3.17) in (3.18) gives eq. (3.19), which enables us to calculate from two values of the control parameter A_n at which bifurcation takes place. In this manner one can proceed up to the value (3.20) at which chaos appears. In fact, this prediction is approximate only; nevertheless, as proved by various experiments [16], the predictions fit the reality quite well.

$$A_4 = \frac{A_2 - A_1}{\delta^2 + \delta} + A_2 \quad (3.19)$$

$$A_\infty = \frac{A_2 - A_1}{\delta - 1} + A_2 \quad (3.20)$$

3.3.6 Self-similarity

Another common feature of chaos is self-similarity [6], a phenomenon which can be seen quite well on bifurcation diagrams. Self-similarity is best demonstrable in fractal geometry. Basically, self-similarity is the property of a geometric object that contains a component part which is identical with or very similar to the geometric structure of the whole object. In other words, a sub-set of the parent object is similar to the parent object. This property is actually only a geometric-linguistic expression

of rather complex mathematical structures and the associated mathematical apparatus which is used in fractal geometry. Self-similarity can be demonstrated graphically on two classic fractal objects - snowflake and fern (Fig. 3.18 - 3.19). Take any part of the object: its structure will resemble that of the basic object.

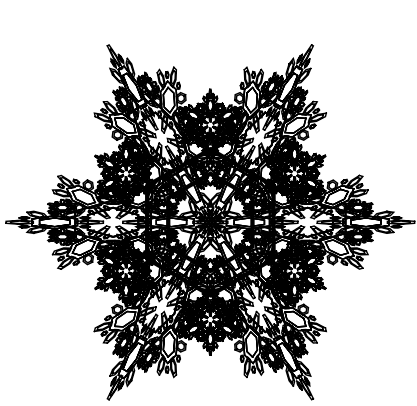


Fig. 3.18 Self-similarity in snowflake ...



Fig. 3.19 ... and in fern.

The same applies, for instance, to bifurcation diagrams. Since their structure is determined by Feigenbaum's constants, which are universal for chaos as such, some graphical visualizations of chaos can be expected to exhibit self-similarity, viz. within a single visualization (a single bifurcation diagram) or among several bifurcation diagrams of different systems. This is well illustrated by the demonstration of self-similarity using bifurcation diagrams (Fig. 3.17). The diagrams clearly display self-similarity. The result will be the same with other bifurcation diagrams also. Self-similarity and other fractal properties can also be found in other visualizations of course (chaotic attractors), but bifurcation diagrams are apparently most graphic for this purpose.

3.4 From Order to Chaos

Deterministic chaos as such does not exist on its own. In fact, it is a type of behavior that can be observed in some nonlinear systems and which can be tackled from various sides. Usually, two methods to get to chaotic behavior are described in the literature: through local bifurcations and through global bifurcations. The two categories are then classed further into special subgroups of transition to chaos. For local bifurcations these include period doubling, quasi-periodicity, and intermittence, the last-mentioned being further granulated into Type I (tangent bifurcation), Type II (Hopf's bifurcation), and Type III (period doubling). For global bifurcations, these include chaotic transients and crises. An overview of the transitions is shown in Table 3.3.

Table 3.3 Ways to chaos

Way to chaos	Note
Local bifurcation	Period doubling, quasi-periodicity, intermittence (type I, II a III)
Global bifurcation	Transients, crisis

Transient to chaotic behavior is very often combination of transients mentioned in the Table 3.3. Complexity of final transient depend on dynamical system structure, but also on the set of signals which influent behavior of given dynamical system.

3.4.1 Period Doubling

Period doubling is another way to reach chaos domain and is joined with so called limit cycles. Term “period doubling” means that under certain conditions is behavior of dynamical system doubling its periodical behavior (from period 2 to period 4, etc...) which is remoted by certain control parameter of observed system. Period doubling is easily observable on so called Poincare section, which is in fact, $N - 1$ dimensional plane through which trajectory is going. All intersections with plane are recorded and are observable like points on Poincare plane, as is depicted at Fig. 3.21, Fig. 3.23 or Fig. 3.25. Under changes of control parameter, system’s trajectory is doubling (number of intersection increase) till chaotic behavior is reached. Period doubling is observable in systems which containing “internal” frequency and are controlled by external signal. In the case that there is no external control input and period doubling is observable, system must contain both signals (frequencies) generated under suitable conditions.

Both frequencies, or better their mutual combination, determine resulting behavior of dynamical system, which is determined by mutual ratios of both frequencies (lets call them for now ω_R and ω_r) which can be rational or irrational. In the case of rational ratio, is resulting trajectory periodical, in the case of irrational ratio one can observe quasi-periodical trajectories. The influence of both frequencies can be easily generated by (3.21). Equations parametrically describe dynamics of trajectory in 3D on a torus, with radius R and r . Frequencies ω_R and ω_r are of rotation around main torus radius R and radius of its body r . On figure 3.20 and 3.21 is depicted trajectory for $\omega_R = 3$ and $\omega_r = 2$ including Poincare’s surface with three points. Trajectory is periodical. For $\omega_r = 2.1$ is trajectory more complicated, see Fig. 3.22 and 3.23. If the raion of both frequencies become to be more irrational, then torus surface is more densely covered and at Poincare section is cutting trajectory creating a circle, see Fig. 3.24 and 3.25.

$$\begin{aligned} x_1(t) &= \cos(t\omega_R)(r\sin(t\omega_r) + R) \\ x_2(t) &= r\cos(t\omega_r) \\ x_3(t) &= \sin(t\omega_R)(r\sin(t\omega_r) + R) \end{aligned} \quad (3.21)$$

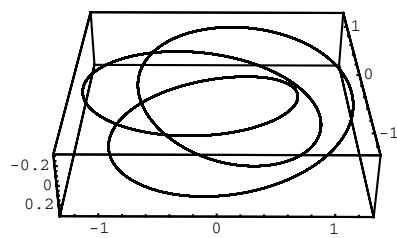


Fig. 3.20 Trajectory and its Poincare section for $\omega_R = 3$

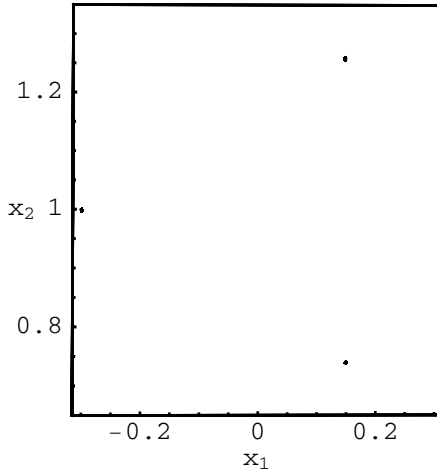


Fig. 3.21 and $\omega_r = 2$

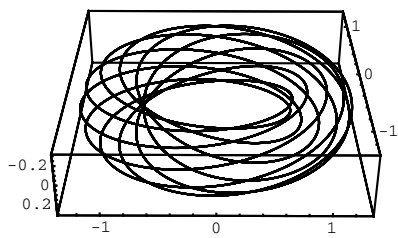


Fig. 3.22 Trajectory and its Poincare section for $\omega_R = 3$

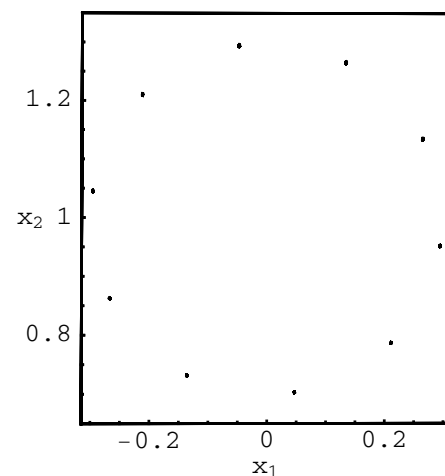


Fig. 3.23 and $\omega_r = 2.1$

If any of the two frequencies is changed, the resulting trajectory need not necessarily be more chaotic; on the contrary, if the two frequencies are in suitable (“more rational”) ratios, “deterministic windows” can appear in the trajectory behavior, i.e. the trajectory does not exhibit chaotic motion. This is demonstrated in Fig. 3.26 - 3.29, where more or less chaotic behavior of the resulting trajectory can be observed

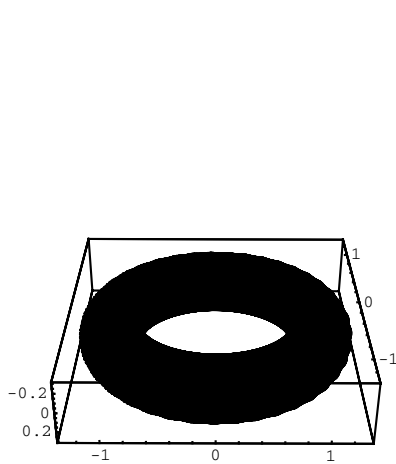


Fig. 3.24 Trajectory and its Poincare section for $\omega_R = 3$

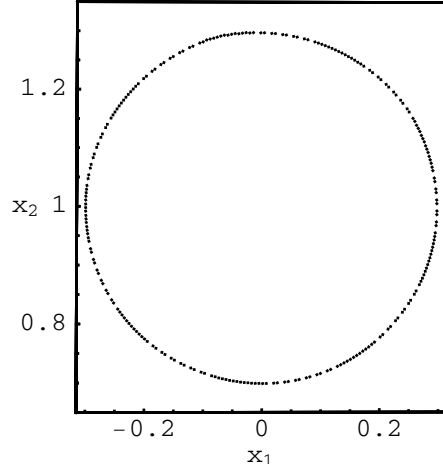


Fig. 3.25 and $\omega_r = 2.33$

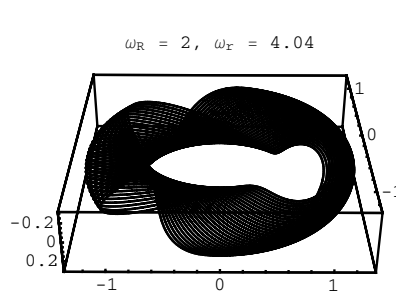


Fig. 3.26 Trajectory for $\omega_R = 2$ and different ω_r

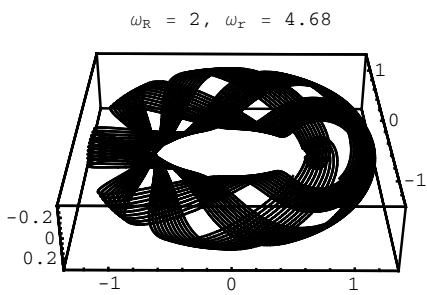


Fig. 3.27 Trajectory for $\omega_R = 2$ and different ω_r

for different. If the behavior becomes chaotic, the trajectory forms a ring, called a drift ring, on the Poincare plane.

The pathway leading to chaos and containing period doubling has the following structure: singular point \rightarrow limiting cycle \rightarrow period doubling \rightarrow quasi-periodicity \rightarrow chaos. Period doubling and quasi-periodicity play the parts of chain links only. Apart from special cases, transition from quasi-periodicity to chaos is only possible if a new, third frequency appears in the system with a constant change in the control parameter. Three dimensions as a minimum are needed for chaos to emerge. If (except for special cases as mentioned) chaos could emerge for less than 3 dimensions, this would be in violation of the Poincare-Bendixon theorem, according to which

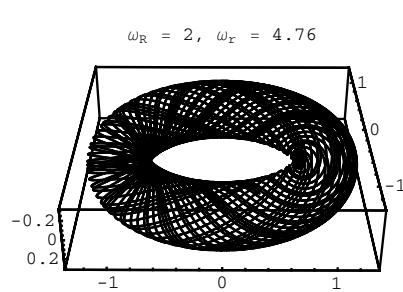


Fig. 3.28 Trajectory for $\omega_R=2$ and different ω_r

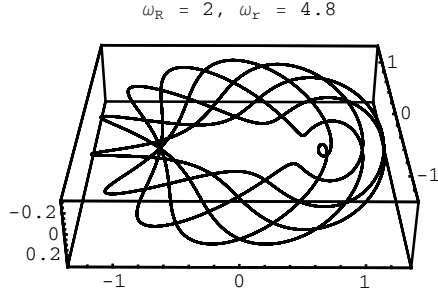


Fig. 3.29 Trajectory for $\omega_R=2$ and different ω_r

chaos cannot emerge in 2D. Period doubling with subsequent quasi-periodicity is a universal phenomenon which can be observed in a wide range of dynamic systems. The only condition that must be met is that a suitable number of frequencies exist in the system, while the physical structure of the system does not matter. When studying the phenomenon of period doubling, the system can be looked upon as pair of systems where one system is superior to (affects - controls) the other system. This is also referred to as oscillator locking (coupling), specifically frequency locking, phase locking or mode locking [16], which are different names for the same phenomenon. The extent of locking is given by the ω_R and ω_r , or more generally by ω_1 and ω_2 in 3.22, frequency ratio, and is denoted w , from the term winding number (also called rotation number).

$$w = \frac{\omega_2}{\omega_1} \quad (3.22)$$

If w is determined by a rational ratio, then the wandering trajectory only forms a finite set of points on Poincare section, and vice versa. It is noteworthy that if the winding number w is plotted in dependence on a suitably chosen system parameter, a fractal called “devil’s staircase” [16], [6] appears. Devil’s staircase for the “circular sine” (eq. 3.23) discrete dynamic system is shown in Fig. 3.30. Meaning of ϕ in eq. (3.23) is such that it is based on general description $\phi_{n+1} = f(\phi_n)$ in which $f(\phi)$ is periodic in angle ϕ , see [16], page 263-265. This staircase is a monotonically increasing curve whose horizontal segments correspond to the winding number (calculated as the ω_R and ω_r frequency ratio) at which frequency locking takes place.

$$\phi_{n+1} = \left\lceil -\frac{K \sin(2\pi\phi_n)}{2\pi} + \phi_n + \Omega \right\rceil \quad (3.23)$$

Period doubling can also be observed in systems whose mathematical model does not directly include any frequency (which does not imply that such a model cannot be set up for the system). Typical examples include the above logistic equation, as demonstrated in Fig. 3.31.

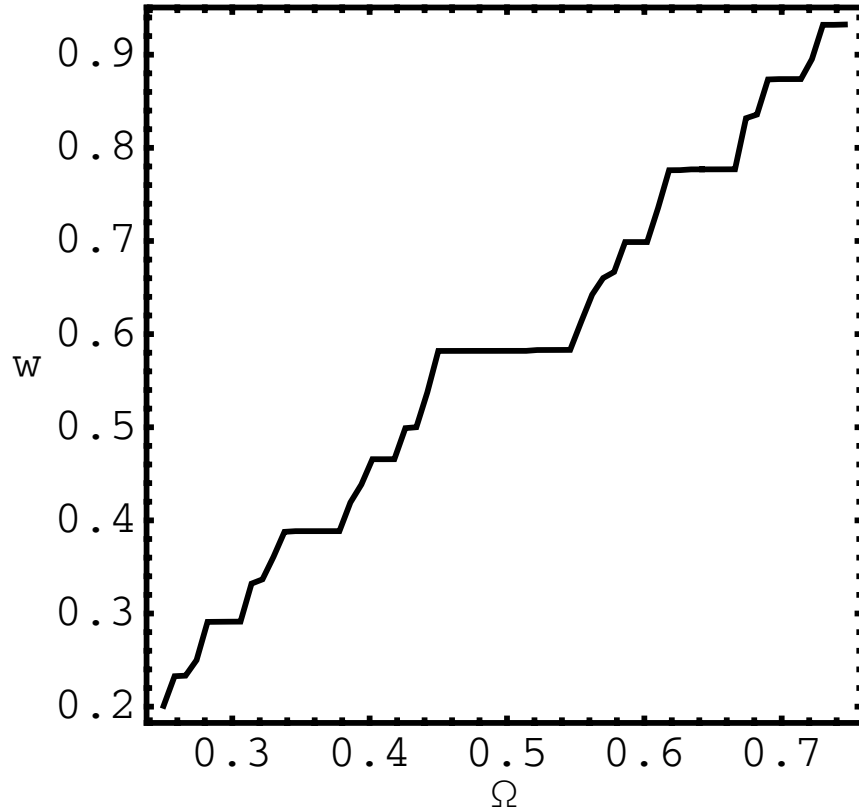


Fig. 3.30 Devil's staircase for the “circular sine” discrete dynamic system with $K = 1.2$ and $\Theta = 0.3$ and $\Omega \in [0.25, 0.75]$

3.4.2 Intermittence

Intermittence is a next pathway to chaos. During this transition to chaos, irregularly appearing regions of chaotic behavior whose length and frequency of occurrence depend on the appropriate system control parameters can be observed in the time development of the system. As the parameters are gradually changed, the chaotic segments can be more and more frequent and ultimately become the only observable behavior of the system (or vice versa). Once again, the behavior of the logistic equation (3.11) can be used to demonstrate intermittence (Fig. 3.14). Intermittence, of both types in which it is usually classed, is seen in both graphs. First type intermittence is a phenomenon where deterministic (periodic) behaviour alternates with chaotic behavior (Fig. 3.14). Second type intermittence is characterized by changes in behavior between chaos and quasi-periodicity (Fig. 3.13). It is noteworthy that in both cases, an object whose apexes fill an imaginary triangle appears in the development roughly at the 30th iteration. This object has its name and is amply used

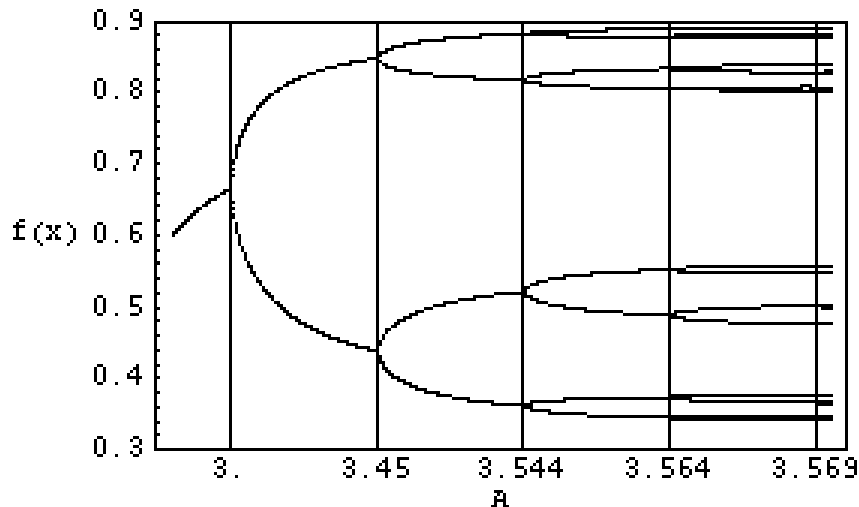


Fig. 3.31 Period doubling in the logistic equation

in stock exchange speculations to predict the near-future behavior of stocks. One of the technical indicators, its name is Triangle.

Generally speaking, intermittence is based on the existence of singular points in the dynamic system's state space. The abrupt dramatic change in the system behavior is due to the fact that some singular points vanish when the control parameter is changed slightly and are not replaced by other singular points. As some singular points vanish, the remaining singular points and their attractivity basins undergo overall position reconfiguration, and as a consequence, a trajectory which was periodic becomes chaotic and vice versa. The reverse phenomenon is also feasible of course, singular points can "be formed", whereupon the state space is reconfigured and the system behavior changes.

The dependence of the existence of singular points on an external control parameter can be well demonstrated on iterative mappings, e.g. on the logistic equation. Fig. 3.32 shows the logistic equation in five-fold iteration for different values of the control parameter A . If $A = 3.74$, this "system" includes some singular points of the sink type, by which trajectories are attracted, and some source type points, by which trajectories are repulsed. In the steady state the behavior can then be deterministic. If the A -values start to change towards 3.72, singular points vanish (no point of intersection with the logistic equation curve with a slope of 45° exists). If the system development reaches this area, it starts to exhibit deterministic behavior, because it cannot do otherwise in the limited space between the slope and logistic equation curve (see Fig. 3.34). Since the intersection of the curve and 45° straight line emerges or vanishes here, this phenomenon is called tangent bifurcation or also saddle-node bifurcation.

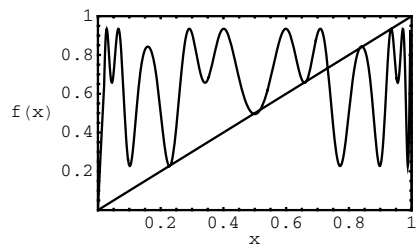


Fig. 3.32 Logistic equation intermittence for $A = 3.7375$

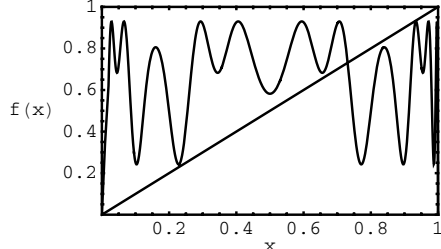


Fig. 3.33 and 3.7427

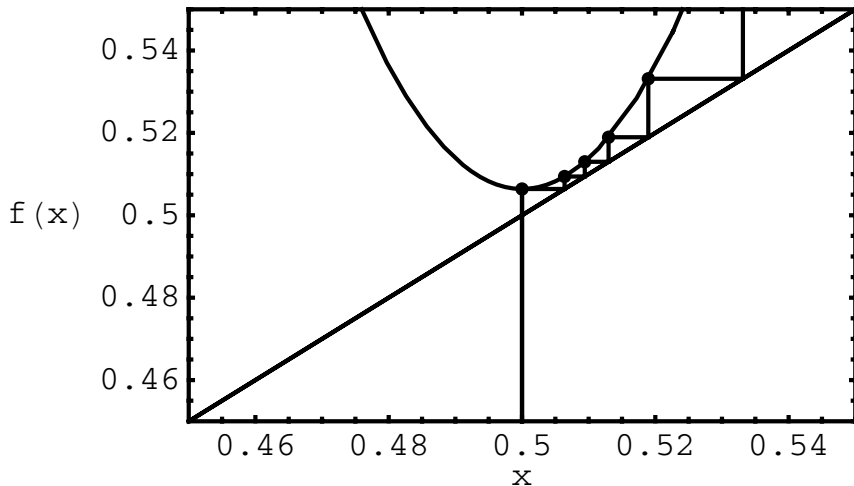


Fig. 3.34 Occurrence of intermittence for the logistic equation with $A = 3.7375$, detail from Fig. 3.33

In this case the logistic equation tends to chaos (Fig. 3.36). If the parameter varied from 3.72 to 3.74, deterministic sequences would be more and more frequent in the chaotic behavior and ultimately the behavior would be purely deterministic. So far it was tacitly assumed that the intermittence was induced by purely deterministic A -parameter setting. In the real world, however, virtually everything is affected by noise, which can superpose control signals as well as other signals. This implies that noise can also affect the A -parameter, which otherwise can also be constant, approaching tangent bifurcation. It will be clear that with a suitable noise intensity and nature, the A -parameter can take values at which singular points vanish, and furthermore, that due to the properties of noise, this value will be transient rather than permanent and that the A -parameter will eventually return to its initial value. The frequency of occurrence of intermittence so induced can be quite different from that obtained by deterministic “excitation”. The effect of noise on the existence or

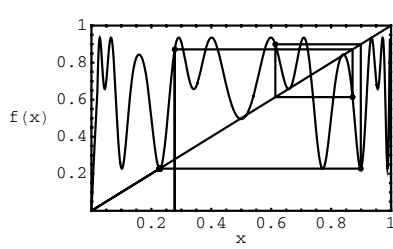


Fig. 3.35 Behaviour of the logistic equation with $A = 3.74$

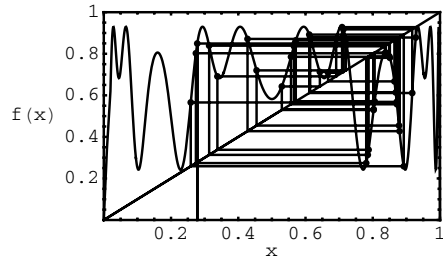


Fig. 3.36 and 3.72, 60 iterations

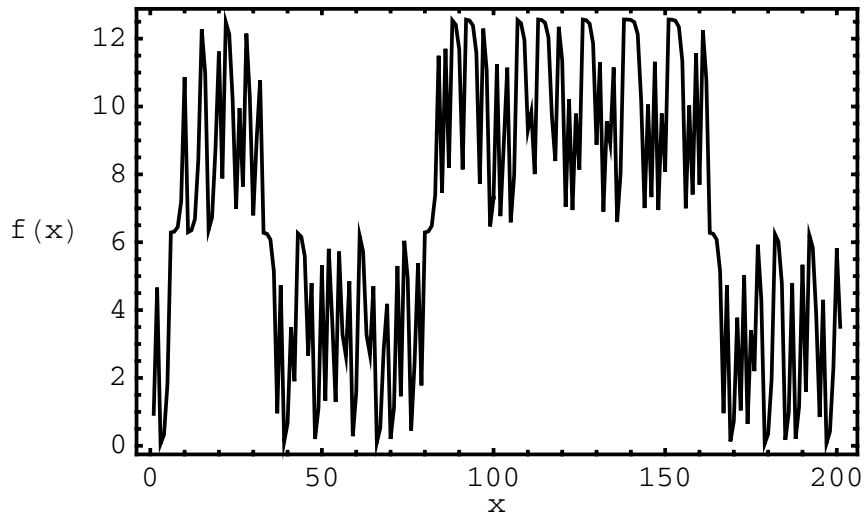


Fig. 3.37 Behaviour of the relation $x_n + 1 = Asin(x_n) + x_n$ at $A = 4.61$ and $x_0 = 0.91$

non-existence of intermittence is a problem which is too complex to be discussed in this publication.

3.4.3 Chaotic Transients

Chaotic transients are a typical phenomenon accompanying models that are based on differential equations. The state space of such a system-model generally includes n singular points lying on the intersections of separatrices dividing the state space into regions with different types of behavior. A state space can generally have N dimensions and so a separatrix may not be a mere curve; instead, it constitutes a smooth, differently wavy plane referred to as manifold. Such manifolds can get, without any collision, as far as the state space boundary or else they can intersect.

The source of deterministic chaos in dynamic systems modeled by differential equations is the manner in which the manifolds intersect and thus separate the state space regions from one another. Two types of manifold intersections exist: homoclinic and heteroclinic. The principle can be best explained on manifolds in 3D with a Poincare plane. An artificial example of manifolds is shown in Fig. 3.38 and 3.39, exhibiting also their Poincare plane. Manifolds are classed into stable manifolds (in-set) and unstable manifolds (out-set). If a state trajectory starts its path on a stable manifold, it is attracted directly into a singular point, whereas repulsion occurs if the manifold is unstable. This also holds for reasonably near manifold neighborhoods. Generally, the nearer a state trajectory is to a manifold, the more its behavior will be affected by that manifold.

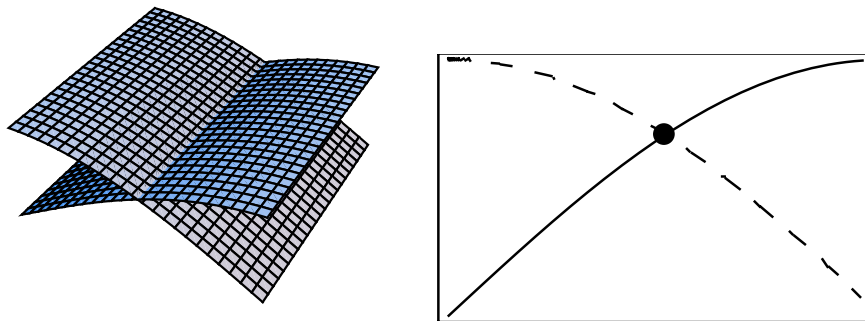


Fig. 3.38 Manifolds in 3D (left) and their Poincare plane

Fig. 3.39 The dashed area represents an unstable manifold

Homoclinic intersection is an intersection of manifolds originating from the same singular point. This is demonstrated in Fig. 3.40 and 3.41 showing a special case of intersection of manifolds which is more interlinking than intersection. Homoclinic intersections, demonstrated in Fig. 3.40 and 3.41, are less common. A classic example is the intersection of manifolds shown in Fig. 3.42, exhibiting what will happen in such case. If two manifolds intersect in this manner, the intersecting manifold will create a set of intersections of which there are infinitely many and whose “density” increases towards the singular point. It will be clear that 3D representation of such intersection creates a much more complex structure - the old state space is broken down and trapped in any regions from which the trajectory cannot escape and an attractor emerges.

The appearance of an attractor is thus determined by the formation of a kind of “pocket” whose boundaries are formed by two manifolds of opposite nature. As explained above, manifolds affect the behavior in their neighborhood. If a trajectory starts its path anywhere within such a region, then it is necessarily attracted by one of the manifolds and repulsed by the other manifold. The moment the trajectory is attracted near to a set of points that appear as a singular point on the Poincare

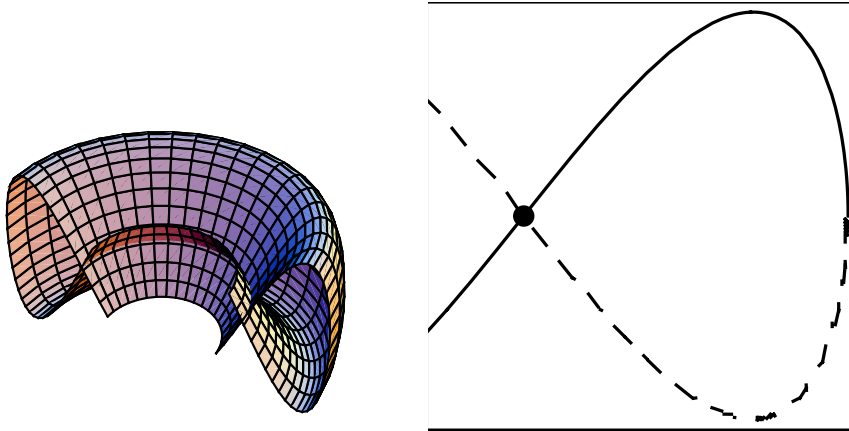


Fig. 3.40 Homoclinic intersection in 3D representation...

Fig. 3.41 and its representation on Poincare plane

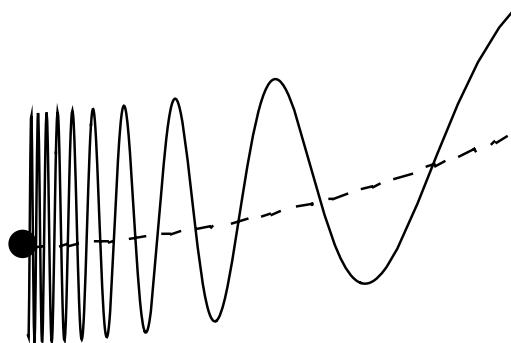


Fig. 3.42 Homoclinic intersection of manifolds - a more common case

plane and forms a homoclinic trajectory in 3D, it is hurled off due to the presence of an unstable manifold. Such a trajectory moves constantly on trajectories which do not repeat. An artificial case of such development is shown in Fig. 3.43 and 3.44. Singular points (and manifolds rising from them) are saddle type, and the chance that the trajectory will start its path precisely in the position of a homoclinic point set is nearly certainly nil. This is contributed to by the ubiquitous noise, inaccuracy of measurement, etc., including quantum uncertainty which is actually transformed as far as to the macroworld.

The Lorenz attractor is a clear example of the emergence of chaos based on intersecting manifolds, we recommend to read for more [13].

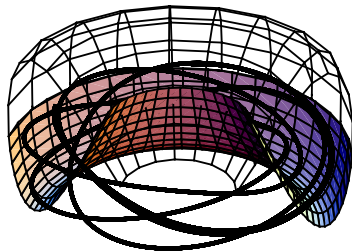


Fig. 3.43 Trajectory in a region bounded by manifolds and by their intersections

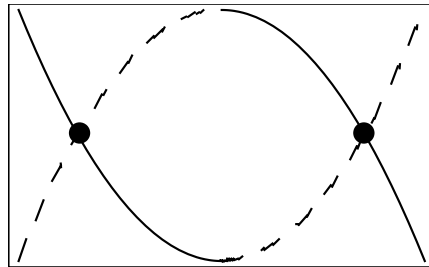


Fig. 3.44 Cut through region from Fig. 3.43

3.4.4 Crises

Crises are a phenomenon where chaotic behavior usually changes dramatically. Such changes can be of various nature. Deterministic behavior can vanish altogether, to be replaced by pure chaos, or conversely, the magnitude of the attractor changes, as does the size of its basin of attraction. Such changes have a common denominator, namely, the quality and configuration of singular points in the state space, including their change in dependence on the control parameters. Crises are categorized into 2 classes: boundary crises and interior crises. Boundary crises occur on imaginary boundaries of attractors, which are determined by a suitable control parameter value. For the logistic equation, the boundary is $A = 4$. Beyond this boundary the chaotic attractor, represented by “snowing” in the bifurcation diagram, vanishes. This is due to the divergence of the trajectory away from the region in which the chaotic attractor was initially present. For the logistic equation with $A = 4$ and $x_0 \in [0, 1]$ the trajectory is confined in the chaotic attractor, because any calculated value of it again lies within the interval of $[0, 1]$, and since it serves as the logistic equation argument in the next iteration, it is clear that such a number would also belong to that interval. However, if A is changed, say, to $A = 4.1$, then levels in excess 1 can be attained in the area of the apex of the parabola generated by the logistic equation. The time needed to attain that area is relatively short. If a trajectory “strays” into that area, it starts running away from the area where the chaotic attractor was initially present at $A = 4$. In other words, if the value is changed to $A > 4$, a “creep-hole” in the chaotic attractor opens up, enabling the trajectory to escape. Such change can be caused by deterministic influences (control, ...) or by random effects (noise). Boundary crisis is demonstrated for the logistic equation in the form of the WEB diagram in Fig. 3.45. When the number of iterations exceeds 11, the trajectory reaches the apex of the parabola and escapes to infinity in this case. Something similar can also be observed on the “circular sine” bifurcation diagram (Fig. 3.46), where chaos vanishes abruptly at $K = 3.8$ and purely deterministic behavior establishes in a different region of the state space (up to a value of approximately 4.27). The same effect can be observed in Hénon bifurcation diagram at $C = 1.8$.

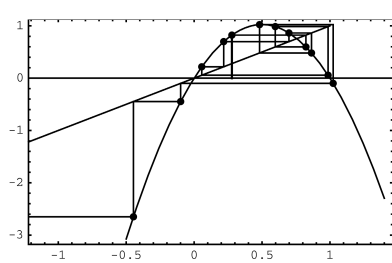


Fig. 3.45 WEB diagram of the logistic equation for $A = 4.1$. Example of boundary crisis

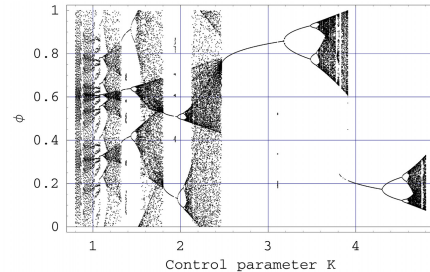


Fig. 3.46 “Circular sine” bifurcation diagram

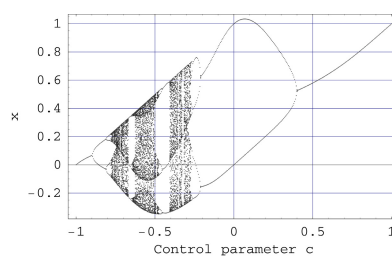


Fig. 3.47 Bifurcation diagram of “Gaussian map” $x_{n+1} = e^{-bx_n^2} + c$

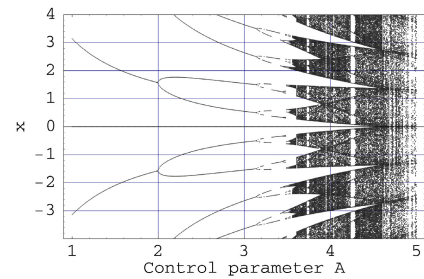


Fig. 3.48 Bifurcation diagram of $x_{n+1} = A \sin x_n + x_n$

Interior crises are changes in behavior during which the chaotic attractor undergoes dramatic changes but does not vanish. The bifurcation diagram of the Gaussian map (Fig. 3.47) is a graphic example showing how the chaotic attractor structure changes in dependence on the control parameter c . The expansion of the chaotic attractor is usually due to collision of a trajectory with a source type or unstable limiting cycle type singular point. In such case the trajectory is “hurled off” to regions where it normally would not get or would get in an extremely long time. Like in intermittences, noise plays an important role in crises.

Due to crises, attractors can be linked up into a single one, or conversely, can decompose into several attractors [25]. Fig. 3.48 shows the behavior of equation $x_{n+1} = A \sin x_n + x_n$ in dependence on A -parameter and different initial conditions. Observing what happens when this parameter is increased, one finds that all attractors are combined into a single one starting from $A \approx 4.603$. Before this level, the trajectory develops in one of the attractors shown only, in dependence on A and on the starting value. The trajectories only merge at $A > 4.603$. Decrease in A is accompanied by the reverse effect - decomposition of the bound attractor into a number of disjoint attractors at $A < 4.603$.

3.5 Selected Examples

Deterministic chaos can be observed in many dynamic systems of different nature. Included are electronic systems (Chua's circuit, circuits with diodes, circuits with digital filters,...), mechanical systems (double pendulum, magnetic pendulum, billiard problem, ...), biological systems (logistic equation, evolutionary dynamics systems, ...), physical systems (physical plasma, the three-body problem, hydrodynamics, ...) and others. Some can be simply materialized on the bench, whereas others can only be observed within a natural process. The objective of this chapter is to demonstrate deterministic chaos on selected examples, specifically from the domains of mechanics, electronics, biology, meteorology and numbers theory.

3.5.1 Mechanical System – Billiard

There are countless examples of deterministic chaos in classical mechanics. A very didactic example is the experiment with small balls falling through a system of bars fixed in a wall. This problem concerns the reflection of two bodies with curved surfaces - balls in this case - or of a radius (beam) from a spherical surface. Taking into account the curvature of the surfaces it will be clear that even the slightest change in the initial conditions will bring about differences in the repeated trajectory. Sensitivity to initial conditions in the billiard problem can be clearly seen on the simulation of falling of a ball through a system of bars with 20 rows (Fig. 3.49). Here the simulation was repeated four times with differences in the initial conditions (x -axis) of 0, 0.00001, 0.00002, and 0.00003, respectively. The difference in the initial conditions

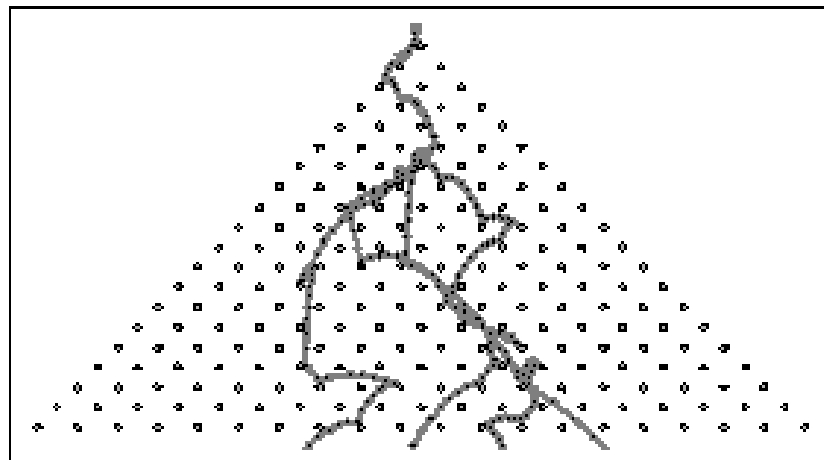


Fig. 3.49 Variant of trajectories in the billiard problem

was thus in the order 10^{-5} . Despite the small number of bar rows (exactly 20) the trajectories are apparently different starting from the seventh row.

The billiard problem can be demonstrated not only on classic balls but also on many other types of “billiard”, which are basically curved surfaces forming together closed objects in which the divergence of colinear radii can be well observed. Another example is at Fig. 3.50. It is clearly visible that trajectories diverge after a few iterations. Starting positions were $x_1 = 0.936578, y_1 = 1.31709$ and $x_2 = 0.936578, y_2 = 1.3063$.

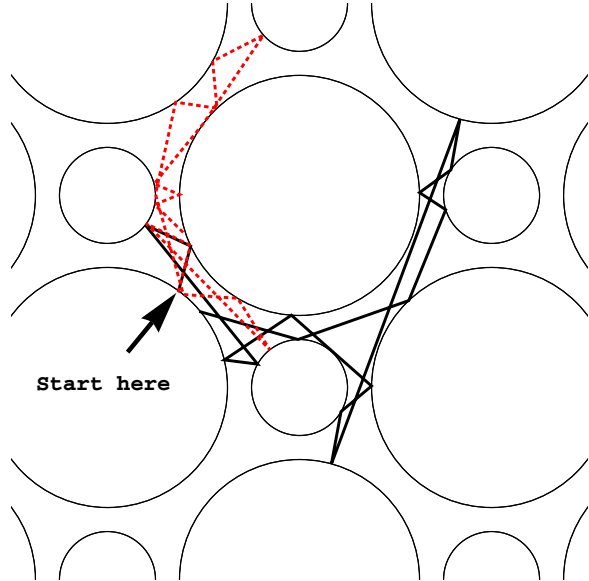


Fig. 3.50 Another variant of the billiard - trajectories diverge after a few iterations. Starting positions were $x_1 = 0.936578, y_1 = 1.31709$ and $x_2 = 0.936578, y_2 = 1.3063$

3.5.2 Mechanical System – Duffing’s Equation

Duffing’s equation describes Duffing’s oscillator, designed in 1918. Duffing’s oscillator consists of a metallic strip with an ac electromagnet located near the centre of the strip. The electromagnetic field which is formed by the magnet displaces the strip sideways. Duffing’s oscillator is modeled by (3.24) which, however, describes the ideal case where no energy is lost. In a real Duffing’s oscillator, energy losses must be taken into account, as in eq. (3.25). This equation transforms into eq. (3.26) for the external excitation setup.

$$\ddot{q}(t) - aq(t) + bq(t)^3 = 0 \quad (3.24)$$

$$\ddot{q}(t) - aq(t) + bq(t)^3 + cq'(t) = 0 \quad (3.25)$$

$$\ddot{q}(t) - aq(t) + bq(t)^3 = f_0 \cos(t\omega_d) \quad (3.26)$$

Equation (3.24) is a starting point for understanding the origin of chaos in this system. The model contains 3 components: acceleration $\ddot{q}(t)$, linear force effect $aq(t)$, and nonlinear force effect $bq(t)^3$. Various types of the steady state can be achieved in the oscillator by varying parameters a and b . The states can be determined by means of the first integral (3.27) of the system, describing total energy of the oscillator. The total energy consists of 2 components: kinetic energy and potential energy, described by the last term and by the remaining terms in (3.28), respectively.

$$\int \dot{q}(t) (-aq(t) + bq(t)^3 + \ddot{q}(t)) dt \quad (3.27)$$

$$-\frac{1}{2}aq(t)^2 + \frac{1}{4}bq(t)^4 + \frac{1}{2}\dot{q}(t)^2 \quad (3.28)$$

The first two terms in (3.28) can be used to set up the potential (Fig. 3.51 and 3.52) describing its dependence on parameter a . If $a > 0$, the oscillator has three equilibrium states - two stable states (minima) and one unstable state (maximum between the two minima). If $a < 0$, the oscillator possesses one stable state only. The minima and maxima in the potential shown represent states to which the oscillator behavior is attracted or from which it is repulsed. If the entire equation (3.28) is considered, the basin of attraction of Duffing's oscillator can be depicted as shown in Fig. 3.53. In the picture, the variables are interchanged according to scheme . Figs 3.53 and 3.54 display both the basins of attraction and the energy equipotentials - points in which the oscillator possesses the same energy.

The plots in Fig. 3.51 - 3.54 differ in that only the components of the potential energy of the first integral were used in Fig. 3.51. The components contained $q(t)$ only and the graph was generated as the $q(t)$ vs a plot. In Fig. 3.53 and 3.54, kinetic

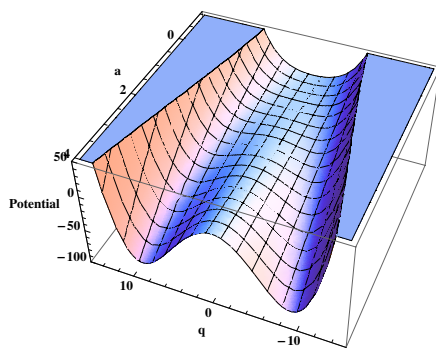


Fig. 3.51 Duffing's equation potential at $b = 0.05\dots$

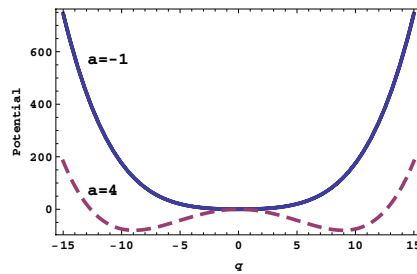


Fig. 3.52 ... and 2D view.

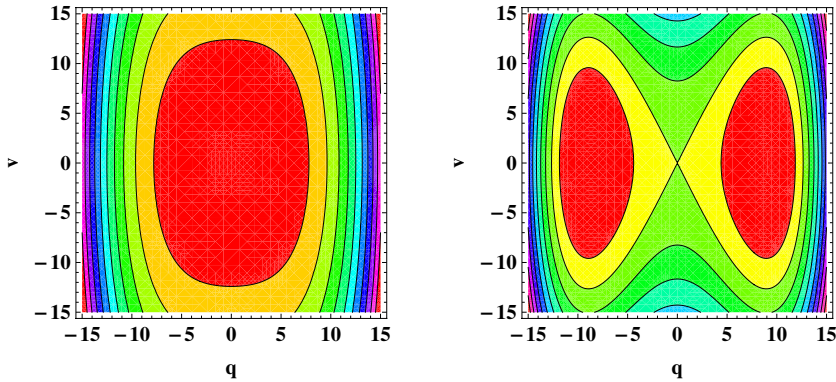


Fig. 3.53 Duffing's equation basins of attraction, $a = -1$ (left) and $a = 4$ (right); $b = 0.05$

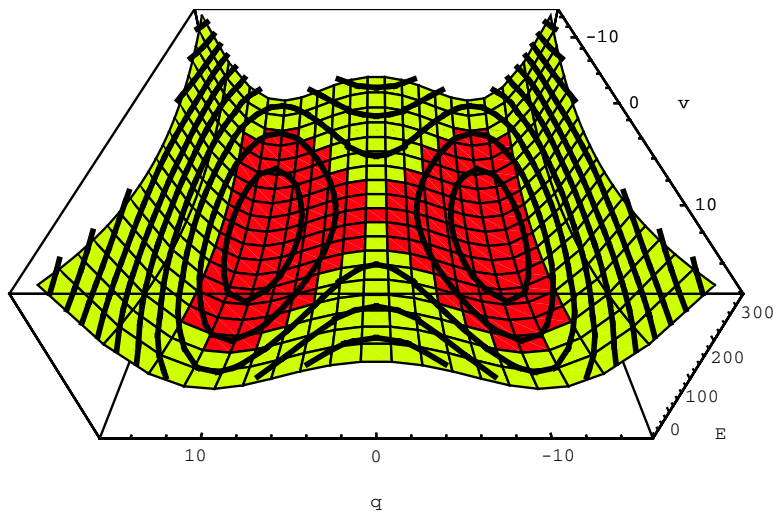


Fig. 3.54 Duffing's equation basins of attraction and equipotentials in 3D for $a = 4$ and $b = 0.05$

energy was also included, enabling non-parametric representation to be applied to the system total energy. The potential in Fig. 3.51 can be imagined as a wire with a ball on it. If the ball is positioned at the local maximum, any impulse can displace the ball from this position. The ball then travels further to some of the sinks, and since friction is not considered in this model, the ball will oscillate about the local minimum infinitely long. If the ball were released from a higher-energy position (level), it would travel cyclically from one local minimum to another through a local energy maximum. If energy dissipation is considered, (3.24) takes the form of (3.25)

where the term $c\dot{q}(t)$ represents dissipation. In this modification the ball motion on the wire will slow down (energy is irreversibly lost) and ultimately stop. Behavior of this type is better represented in terms of the state space and state trajectories. For this purpose, eq. (3.24) is modified to the form (3.29).

$$\begin{aligned}\dot{p}(t) - aq(t) + bq(t)^3 &= 0 \\ \dot{q}(t) &= p(t)\end{aligned}\quad (3.29)$$

In this manner the n_{th} order differential equation is transformed into n first-order equations. The corresponding variables then represent state variables. This system of differential equations can serve to simply draw a “state portrait” (Fig. 3.55) in which the arrows show the direction of the state trajectory (corresponding, in fact, to the equipotential lines in Fig. 3.53 and 3.54). Different types of behaviour of Duffing’s equation with dissipation can be obtained by solving (3.25), in dependence on the extent of dissipation and on initial energy.

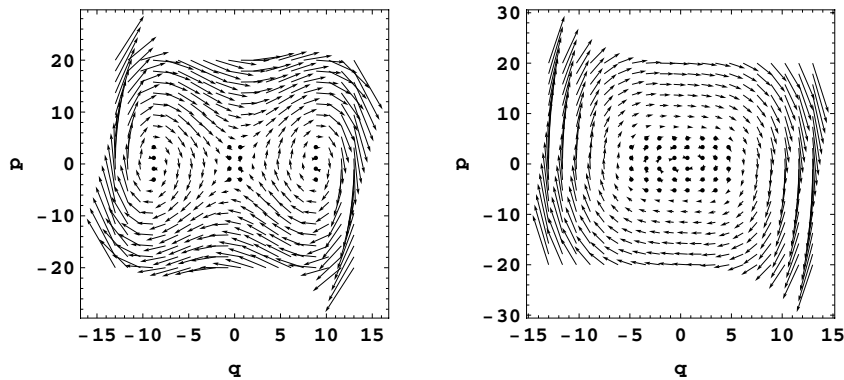


Fig. 3.55 State portrait of Duffing’s equation, $a = -1$ (left) and $a = 4$ (right); $b = 0.05$

It is clear from Fig. 3.56 and 3.57 that the oscillator’s ultimate steady state depends both on initial energy and on initial position, in other words, on initial conditions. The trajectories of the system behaviour are attracted to one of the basins of the system’s state space (Fig. 3.58). Fig. 3.59 - 3.61 shows both the state portrait and the system behavior of eq. (3.25). The gradual energy loss causes the trajectory to “sink” slowly to one of the attractors. In this manner the state space is divided into basins in which the state trajectory gets into one or another attractor lobe. Geometric appearance of such basins can be very complex. See for example system Fig. 3.62 and 3.63 where are depicted basins of attraction with clear fractal border. Black area is the domain of attraction, i.e. if arbitrary trajectory start in it, then will end in white attractor depicted inside black area, otherwise it goes out of the basin. Other color layers represent trajectory “speed” of escaping.

Chaotic behavior of Duffing’s oscillator by can be obtained by choosing suitable excitation conditions. This is described by (3.26). The right-hand side excitation

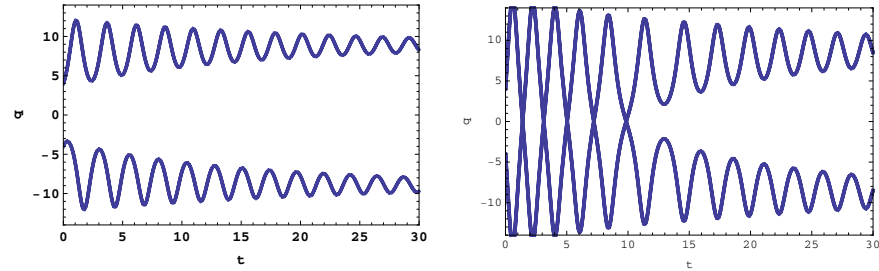


Fig. 3.56 Behavior of Duffing's equations with dissipation...

Fig. 3.57 ... another level of dissipation.

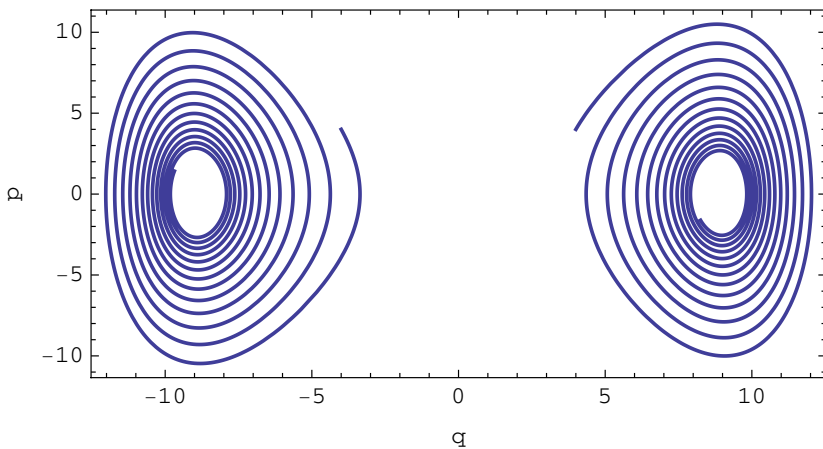


Fig. 3.58 State trajectories of Duffing's equation with dissipation

term consists of the term $f_0 \cos(t\omega_d)$. Both deterministic and chaotic behavior can be observed for Duffing's equation for certain values of the two terms. A typical example of chaos is shown in Fig. 3.64 - 3.65. If the above setup of a ball on a wire is “transformed” into the setup of a ball rolling on a plane, then the appearance of chaos can be understood so that external excitation by the element $f_0 \cos(t\omega_d)$ provides sufficient energy not only to cover dissipation losses but also for chaotic motion of the ball.

3.5.3 Electronic System – Chua’s Circuit, Circuit with a Diode

Electronic circuits are among the most popular systems used to demonstrate deterministic chaos. Their popularity stems from the fact that electronic circuits are easy

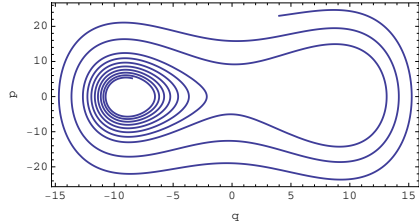


Fig. 3.59 State trajectories of Duffing's equation with dissipation.

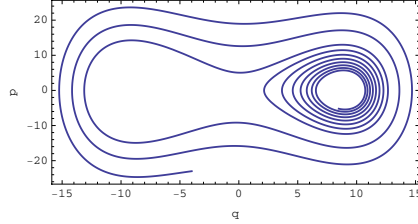


Fig. 3.60 ... another level of dissipation.

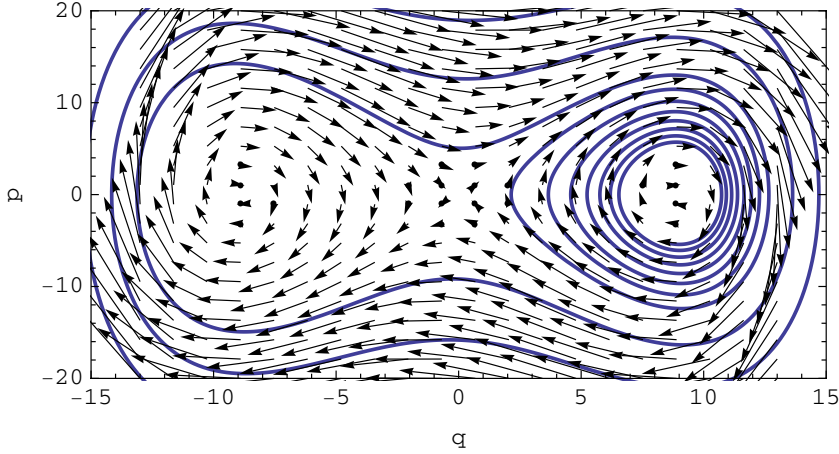


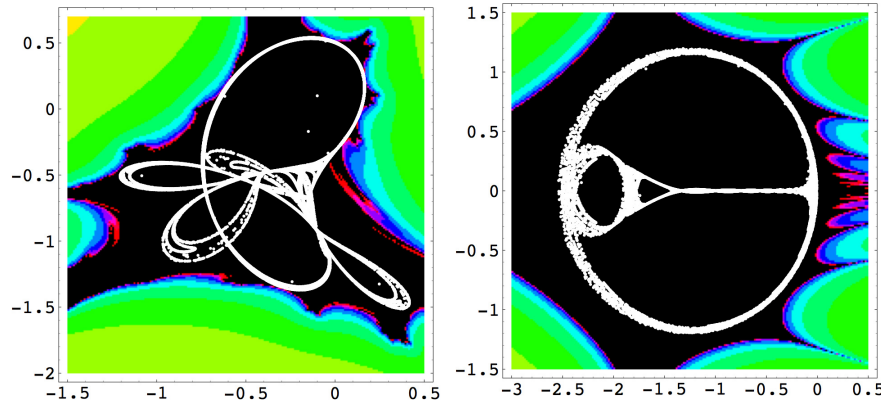
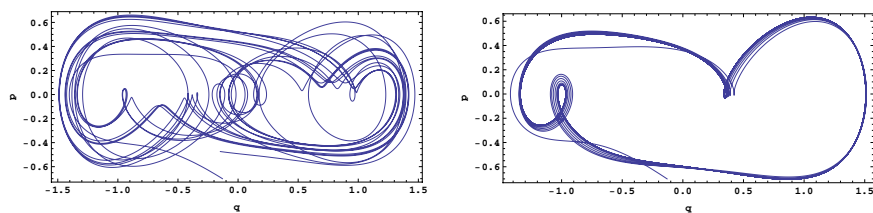
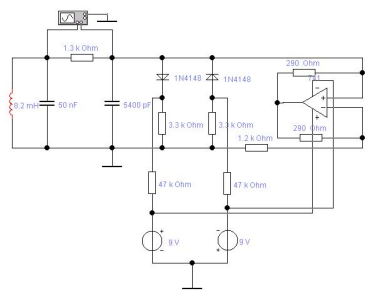
Fig. 3.61 State trajectories of Duffing's equation with dissipation

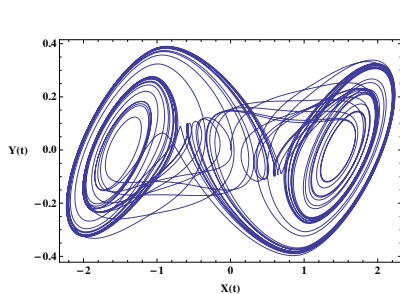
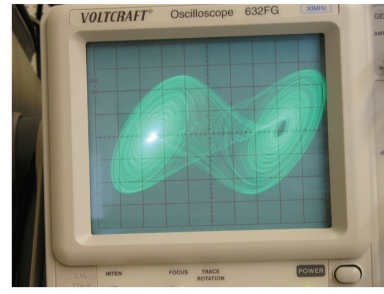
to set up and provide fast response to impulse. Typical representatives of electronic circuits with deterministic chaos include Chua's circuit, whose hardware design and behaviour are shown in Fig. 3.66-3.67 and Fig. 3.68-3.69, respectively. The core of Chua's circuit is a nonlinear resistor, eq. 3.32, sometimes called Chua's diode [33].

On Fig. 3.69 Chua's attractor visualized by the program Mathematica (left) and on the oscilloscope connected to its hardware implementation shown in Fig. 3.67 (left) Chua's circuit can be described mathematically by eq. (3.30), which can be used to simulate the behavior of the circuit:

$$\begin{aligned} C_1 v \dot{c}_1(t) &= G(vc_2(t) - vc_1(t)) - g(vc_1(t)) \\ C_2 v \dot{c}_2(t) &= G(vc_1(t) - vc_2(t)) + i_L(t) \\ L \dot{i}_L(t) &= -vc_2(t) \end{aligned} \quad (3.30)$$

$$vc_1(0) = 0.15264, vc_2(0) = -0.02281, i_L(0) = 0.38127 \quad (3.31)$$

**Fig. 3.62** Example of basin of attraction**Fig. 3.63** Another example of basin of attraction**Fig. 3.64** Duffing's equation chaos for $f_0 = 0.29$ **Fig. 3.65** ... and for $f_0 = 0.32; \omega_d = 1$.**Fig. 3.66** Scheme of the Chua's circuit ...**Fig. 3.67** ... and hardware design of Chua's circuit.

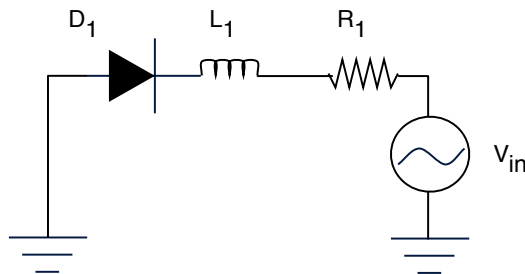
**Fig. 3.68** Simulation of the Chua's circuit ...**Fig. 3.69** ... and the real behavior.

where the nonlinear resistor $g(x)$ is represented by (3.32),

$$g(x) = m_0x + \frac{m_1 - m_0}{2}(|x + b_1| - |x - b_1|) + \frac{m_2 - m_1}{2}(|x + b_2| - |x - b_2|) \quad (3.32)$$

If suitable initial conditions are set as described by (3.31), a chaotic attractor can be found in the system (Fig. 3.68).

A simple electronic circuit (Fig. 3.70) where an excitation source, resistor, coil and diode are connected in series can serve as a next example. The diode provides nonlinearity which is the cause of chaotic behavior in this circuit.

**Fig. 3.70** Layout of the circuit with a diode

The mathematical model of this physical system consists of a system of equations and initial conditions (3.33) where the diode is modeled by means of a piecewise linear capacitance, namely:

$$\begin{aligned} \dot{q}(t) &= i(t) \\ L_1 \dot{i}(t) &= v \sin(2\pi ft) - \left(\frac{|q(t)|(C_2 - C_1)}{2C_2 C_1} + \frac{|q(t)|(C_2 + C_1)}{2C_2 C_1} + e_0 \right) + i(t)(-R_1) \\ q(0) &= 0 \\ i(0) &= 0 \end{aligned} \quad (3.33)$$

Chaotic behavior can be observed when analyzing the dependence of charge q on control voltage V . Numerical simulations of this circuit are shown in Fig. 3.71 and 3.72, displaying the time development of the behavior of the circuit, and in Fig. 3.73 and 3.74 displaying the behavior of the dependence of current i on $q(t)$.

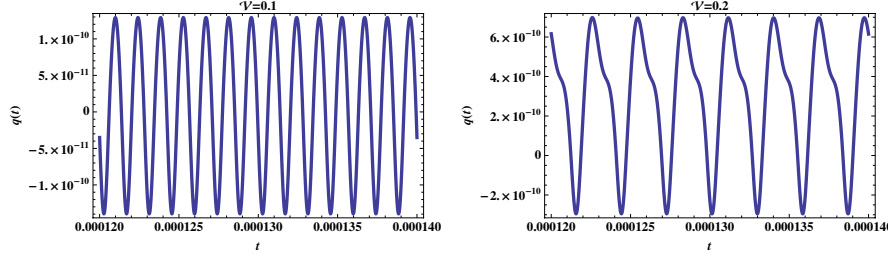


Fig. 3.71 Simulation of the diode circuit ...

Fig. 3.72 ... for different values of v .

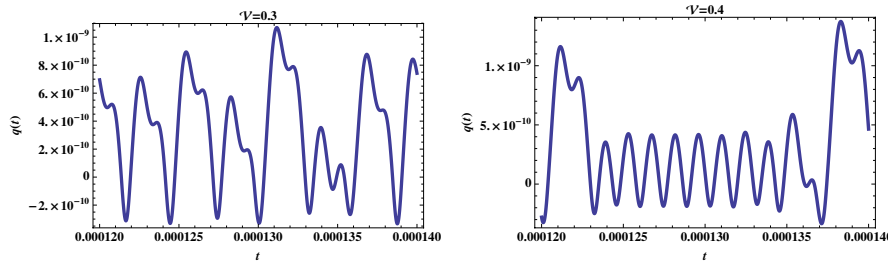


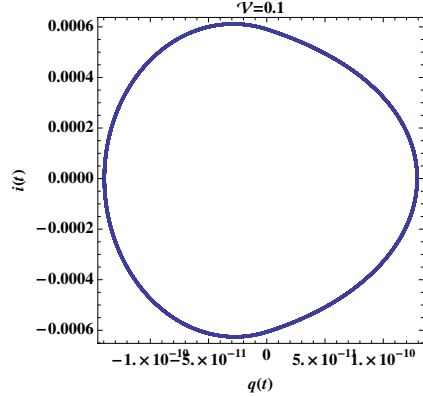
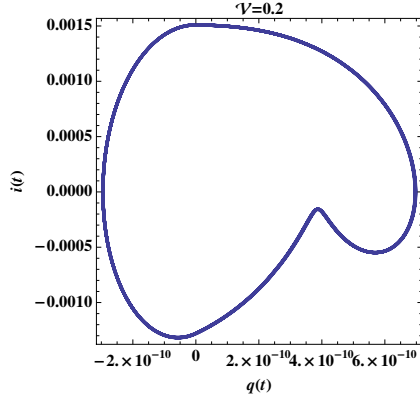
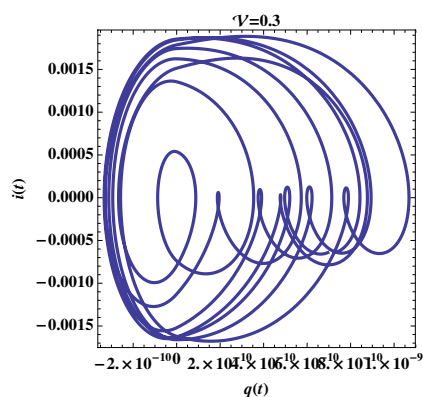
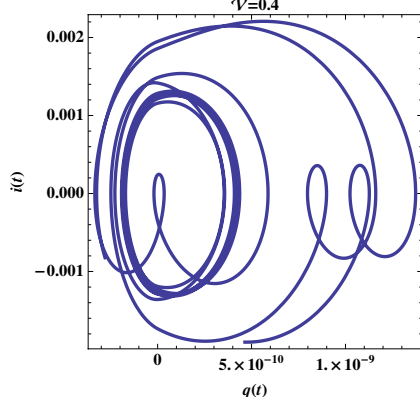
Fig. 3.73 Simulation of the diode circuit ...

Fig. 3.74 ... for different values of v .

The bifurcation diagram of the circuit with a diode is shown in Fig. 3.79. The diagram clearly displays transition to chaotic behavior with increasing parameter V . From the structure of the bifurcation diagram one can not only see structure repetition (self-similarity) but also the fact that all three parts are visually very similar to bifurcation diagrams of the logistic equation (Fig. 3.81), which is just another evidence in a series of experimental evidences of universality of chaos as such.

3.5.4 Biological System – Logistic Equation

The logistic equation is the most typical example in the domain of biological systems. This equation models the evolution of dynamic co-evolutionary systems of the predator-prey type in which all the relevant behavior types are present. The logistic equation is modeled by relation eq. (3.34). An important element in this equation is the control parameter A , whose gradual change in the equation gives rise to behavior

Fig. 3.75 Dependance of i on $q(t)$...Fig. 3.76 ... for different values of v .Fig. 3.77 Dependance of i on $q(t)$...Fig. 3.78 ... for different values of v .

which can be visualized conventionally (Fig. 3.80) or by means of the bifurcation diagram (Fig. 3.81). Logistic equation is a suitable tool for studying the transition from deterministic behavior to chaotic behavior as well as phenomena accompanying that transition, such as intermittence and period doubling. Recall that logistic equation takes the form

$$x_{n+1} = Ax_n(1 - x_n) \quad (3.34)$$

Fig. 3.80 shows chaotic behavior of the logistic equation for precisely defined initial conditions and control parameter A . The behavior depends both on the initial conditions and on the control parameter, as the two bifurcation diagrams in Fig. 3.81 clearly demonstrate.

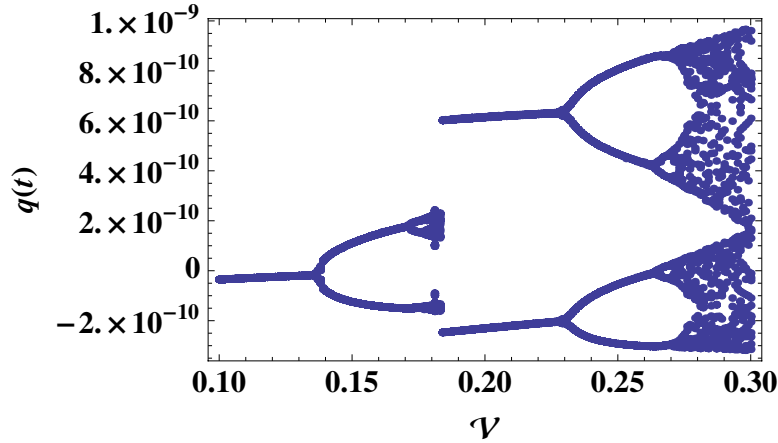


Fig. 3.79 Circuit with a diode - bifurcation diagram

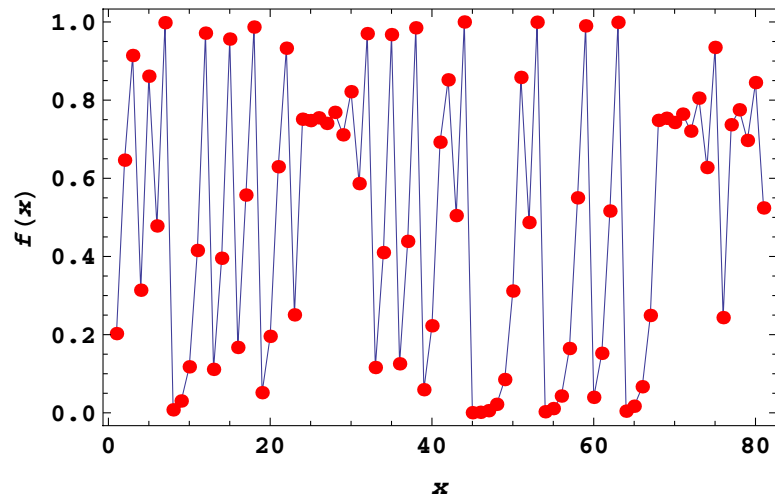


Fig. 3.80 Behavior of the logistic equation in time for $A = 4$, $x_0 = 0.2027$

The diagrams show the chaotic patterns of the system behavior in dependence on the control parameter. We would like also to note that the bifurcation diagram (and bifurcation in general) is related to abrupt changes in the system behavior, referred to as catastrophes, in dependence on the control parameter (Thom's catastrophe theory, see also [13], [4], [21]).

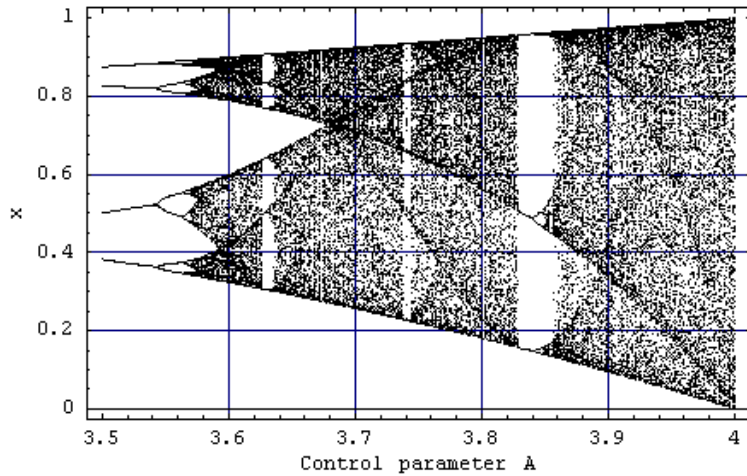


Fig. 3.81 Bifurcation diagram of the logistic equation

3.5.5 Meteorological System – Lorenz Weather Model

A typical representative of deterministic chaos is a very simple model of the behavior of weather expressed by a system of equations devised by Edward Lorenz at MIT in 1963. Lorenz is generally regarded as the discoverer of deterministic chaos. The equations, including the initial conditions, are given by (3.35). They represent a hydrodynamic model of the behaviour of a gas or liquid during external heating [16]. A simulation of (3.35) provides the chaotic attractor that is shown in Fig. 3.82-3.83.

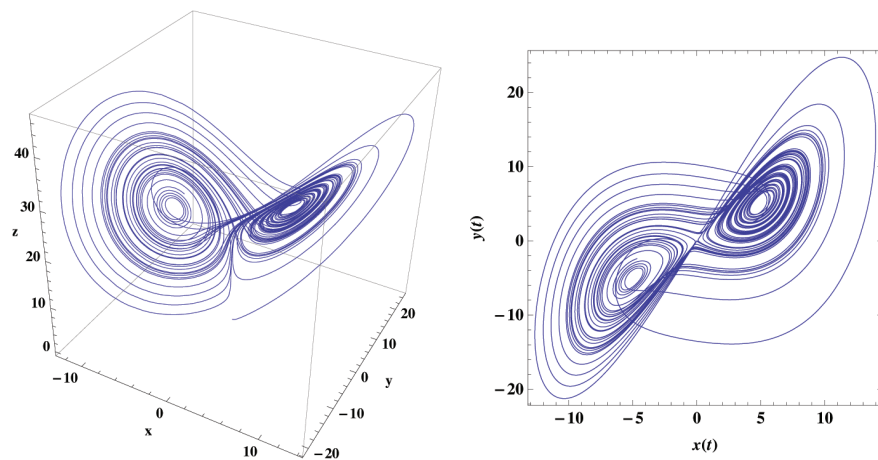


Fig. 3.82 The Lorenz attractor in 3D ...

Fig. 3.83 ... and 2D representation.

The attractor consists of two lobes in whose centers are singular points that attract trajectories from their neighborhood and, after certain attraction, repulse them away. The arrangement of the two singular points is such that the repulsed trajectories get into the attraction domain of the opposite singular point, where the process is repeated.

$$\begin{aligned}\dot{x}_1(t) &= -a(x_1(t) - x_2(t)) \\ \dot{x}_2(t) &= -x_1(t)x_3(t) + bx_1(t) + x_3(t) \\ \dot{x}_3(t) &= x_1(t)x_2(t) - x_3(t)\end{aligned}\quad (3.35)$$

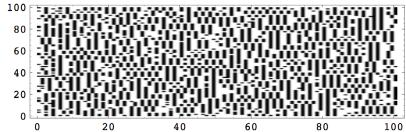
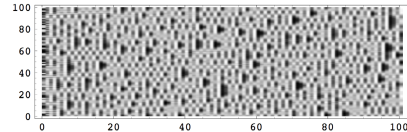
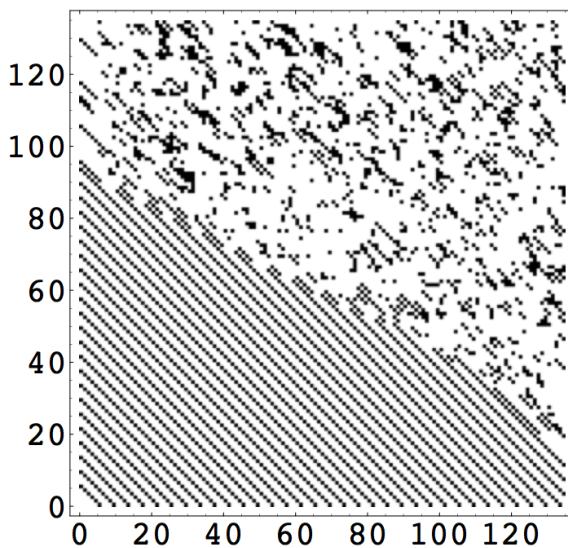
The origin of the Lorenz attractor, including modifications in the nature and positions of the singular points, is described in detail in [13]. It should be noted that the accuracy of calculation of the behavior of a chaotic system also depends on the software and method used.

3.5.6 Spatiotemporal Chaos

The systems discussed so far demonstrated deterministic chaos in the time domain, i.e. where chaotic behavior can be observed in the system behavior developing in time. In addition to this type of chaotic behavior, another type exists, see spatiotemporal behavior ([16], [24]), occurring in systems that are described, e.g., by partial differential equations. Hence, they are systems with distributed parameters. This type of behavior can be nicely and simply demonstrated on the logistic equation discussed above (other iteration equations can also be used, of course) in parallel connection, referred to as Coupled Map Lattices (CML). This is a spatiotemporally coupled system with the development of n equations that affect each other via a coupling constant, usually denoted ε . CML can be regarded as a field of kind of “oscillators” which affect each other. Mathematical description of a CML using an iteration equation for its activity consists in (3.36) where the function which is denoted $f(\dots)$ represents the iteration equation.

$$x_{n+1}(i) = (1 - \varepsilon)f(x_n(i)) + \frac{\varepsilon}{2}(f(x_n(i-1)) + f(x_n(i+1))) \quad (3.36)$$

Equation (3.36) is referred to as a symmetric CML because the k th equation acts on its neighbors (through the coupling constant ε) equally on both sides. Asymmetric CMLs whose description is, naturally, slightly modified, also exist. Such types of relatively simple spatiotemporal chaotic systems provide a very wide scale of behavior, which is used for modelling this type of chaos as well as for the study of its control and use in information transmission and encoding. Figs 3.84 to 3.85 show the behavior of a CML according to eq. (3.36) where term $f(\dots)$ is replaced by the logistic equation, or more precisely by 100 logistic equations that affected each other during 100 iterations. In Fig. 3.84, black points denote values exceeding the level of 0.88 (according to [24]). The other points remain white, due to which information regarding the actual diversity of the spatiotemporal chaos is lost. This is demonstrated by Fig. 3.85, where a gray-scale picture is depicted. Fig. 3.86 shows

**Fig. 3.84** CML in black-white visualization...**Fig. 3.85** ... and its gray-scale version.**Fig. 3.86** 2D CML

another version of CML: 2D version, i.e. both axes x and y are logistic equations joined together. Time line is axe z , which is not visible in Fig. 3.86, this figure is basically only slice cut of 2D CML in iteration 200.

Naturally, CML is not the only method to simulate spatiotemporal chaos. Considerably more complex descriptions (as regards mathematical formalism and solution) exist and will be discussed in the Chapter 6, dealing with the control of chaos.

3.5.7 *Cellular Automata – Game of Life*

Cellular automata [31] represent a tool that can be employed to simulate extensive or complex systems. The history of cellular automata can be traced back to ancient China, specifically to the year 1303. This is the era of origin of the Chinese arithmetic triangle, better known as Pascal's triangle (after the French mathematician Blaise Pascal, 1623 - 1662) published in 1527, which indirectly led to

the later development of probability theory. Cellular automata only enjoyed boom with the development of PCs, which enabled their use in virtually any branch of human activity. Among applications of cellular automata are, for instance, simulation of forest fires, differentiation of cells in human body (Kuffman's model), the human body's immune failure, hydrodynamic phenomena (e.g. motion of particles of a fluid, was used to simulate the behavior of 4 million molecules) and passage of a liquid through unordered geometric structures such as sand. Given the computational capacity of currently available hardware, cellular automata appeared to be so to say predestined for technically demanding "parallel" simulations of systems such as the flow of molecules of a liquid or gas, etc. In such "huge" simulations cellular automata feature simplicity as well as a high speed as compared to conventional calculations. Cellular automata can also be used to simulate tessellations, i.e. mosaics, which find application in investigations into the creation of mosaics in various materials, the shape of boundaries of territories of various predators or the propagation of epidemics. A cellular automaton can be imagined as a grid/matrix, where each square/matrix element represents a cell. In simple automata all cells are subject to a single law, owing to which the most bizarre images can emerge. Apart from their geometrical meaning, such images can provide information about the dynamics of the process involved. If a phenomenon is simulated which is not homogeneous or isotropic (which means identical properties in all points and directions), then this fact must be taken into account when formulating the rule governing the cellular automaton. Among the best known and most popular cellular automata is Game of Life, governed by a very primitive rule and still exhibiting very complex behavior. The rules are very simple and are identical for all cells:

- Any live cell with more than three live neighbors dies, as if by overcrowding.
- Any live cell with fewer than two live neighbors dies, as if caused by under-population.
- Any dead cell with exactly three live neighbors becomes a live cell.
- Dead cells are shown in white, live cells shown in black.

This simple set of rules gives rise to incredibly complex behavior (Fig. 3.88) forming groups of cells that die and become live cells again (blinkers), travel along the cellular automaton (gliders), shoot down gliders (guns) or travel leaving blinkers in their traces (star ships). Cellular automata generate both chaotic behavior and deterministic behavior (Fig. 3.88). The above CML simulation can also be considered a cellular automaton based on eq. (3.36) which is the single rule for all cells here.

3.5.8 Artificial Intelligence – Neuron Networks

Neuron networks - biological or artificial - represent another chaos-generating system. The presence of chaos in biological networks is associated with diseases such as epilepsy, in artificial networks, with the phases of learning and recollection. A neuron network [7] can be represented by an oriented graph whose nodes are neurons, i.e. simple computational units performing primitive mathematical operations

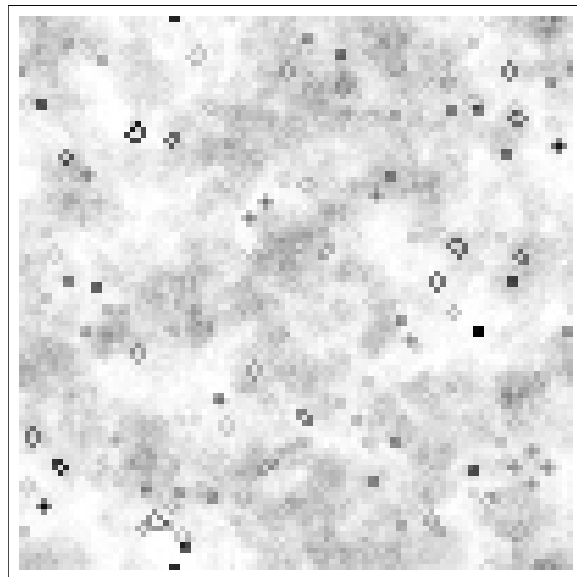


Fig. 3.87 Game of Life containing both deterministic and chaotic structures

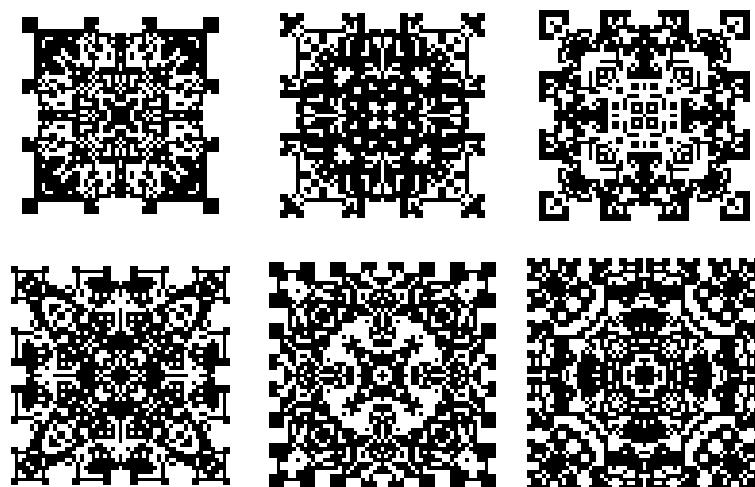


Fig. 3.88 Order in a cellular automaton

such as summation, multiplication, etc. Since a network is formed by discrete objects, it can be looked upon as a special type of cellular automaton, with a special set of cells (input and output neurons). Hence, it is reasonable to expect information

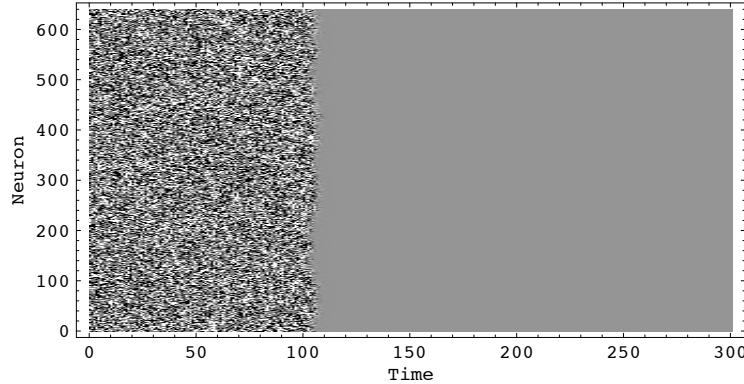


Fig. 3.89 Steadying of chaos generated by a neuron network ($w \in [-0.3, 0.3]$)

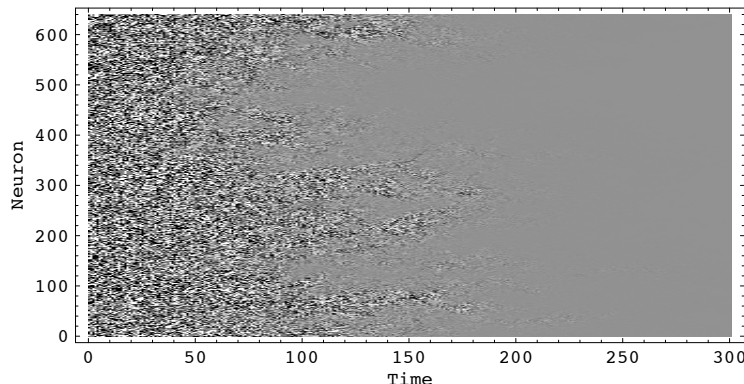


Fig. 3.90 “Intermittence” in the behavior of a neuron network ($w \in [-0.6, 0.6]$)

processing by neuron networks to be accompanied by chaotic behavior. This was confirmed both experimentally (association with epilepsy found) and by simulations (numerical studies on various models). By way of example, consider a simple network [25] which is defined by (3.37). This is a single-layer network where outputs from neurons not farther than r enter the i_{th} neuron. Hyperbolic tangent is the transfer function [7] and w is weight, which is generated at random. Fig. 3.89 to 3.91 display the network’s behavior for identical initial conditions with differently large intervals at which weights w were generated. The color of each point represents the state of the neuron, of which there are 640. Fig. 3.89 clearly demonstrates that starting from an initial chaotic state, all neurons will ultimately assume the same value. It is clear from Fig. 3.90 and 3.91 that even a slight change in the weight generating

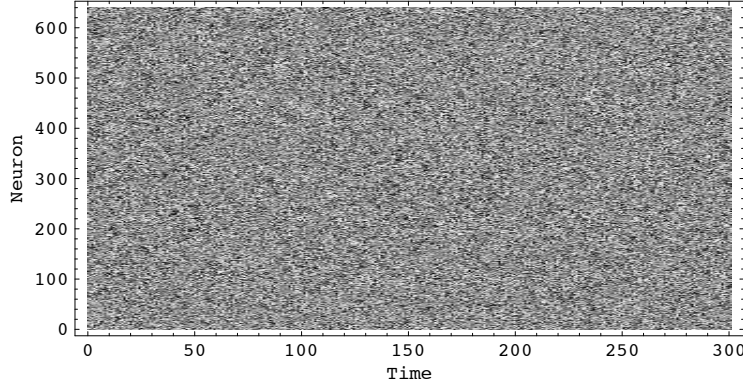


Fig. 3.91 Chaos generated by a neuron network ($w \in [-0.9, 0.9]$)

interval brings about non-uniform stabilization, and regions can be observed where neurons pass from a chaotic regime to a steady-state regime and back (see the group of neurons around neuron 100-150 in Fig. 3.91) - a situation called intermittence. When the interval for weight generation is extended again, the network's behavior is free from any determinism and the networks is in the chaotic regime:

$$x_{n+1}(i) = \tan \left(\sum_{j=1}^r w_i (x_n(i-j) + x_n(i+j)) \right) \quad (3.37)$$

3.5.9 Artificial Intelligence – Evolutionary Algorithms

Optimization algorithms are powerful tools in solving many problems in practical engineering. They are typically used where solving a problem by an analytical method is inappropriate or infeasible. Suitably implemented, optimization algorithms can be used without frequent user interventions into the performance of the facility where they are used. The majority of problems in engineering practice can be defined as optimization problems, such as finding the optimal trajectory for a robot, optimal pressure vessel wall thickness, optimal controller parameter setting, optimal relation between fuzzy sets, etc. In other words, the problem to be solved can be transformed into a mathematical problem defined by a functional prescription whose optimization leads to the finding of arguments of the objective function, which is the goal of the optimization exercise. A number of highly efficient algorithms were developed during the past two decades, enabling highly complex problems to be solved very efficiently and effectively. This class of algorithms has a specific name of evolutionary algorithms. Such algorithms are capable of solving highly complex problems quite well, owing to which they are widespread and popular in many fields of technology. A typical feature of evolutionary algorithms is that

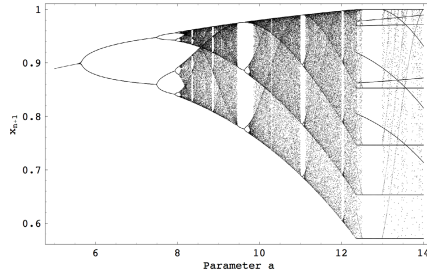


Fig. 3.92 Bifurcation diagram of simple genetic algorithm for $a \in [4, 15]$, $b = 1$, $T = 7/8$

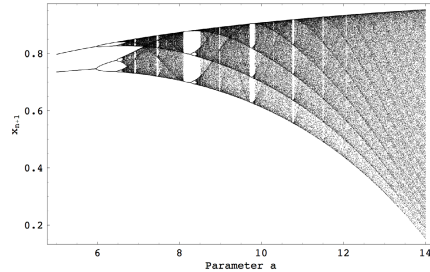


Fig. 3.93 Bifurcation diagram of simple genetic algorithm for $a \in [4, 15]$, $b = 7$, $T = 7/8$

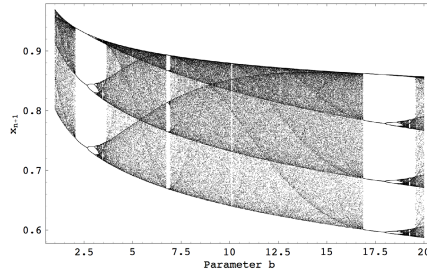


Fig. 3.94 Bifurcation diagram of simple genetic algorithm for $a = 9$, $b \in [1, 20]$, $T = 7/8$

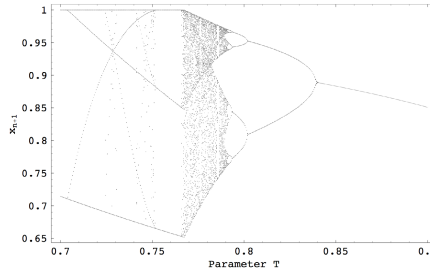


Fig. 3.95 Bifurcation diagram of simple genetic algorithm for $a = 4$, $b = 1$, $T \in [0.7, 0.9]$

they work on populations of possible solutions, called individuals. Such individuals affect each other's quality based on certain evolutionary principles in cycles, usually bearing the name "Generation".

Deterministic chaos has been also observed, mathematically proven and numerically demonstrated in evolutionary algorithms, especially in genetic algorithms as reported in [32].

In that research, dynamical system models of genetic algorithms were considered with the expected behavior of the algorithm analyzed as the population size goes to infinity. Their work is based on the research of [28], [29] and [27]. An elegant theory of simple genetic algorithms is based on random heuristic search on the idea of a heuristic map G . An important point of the research in [32] is that the map G includes all of the dynamics of the simple genetic algorithm, based on eq. 3.38 (truncation selection) and eq. 3.39 (mutation heuristic function). It is defined by $G_{a,b,T} = F_T \circ U_{a,b}$. In both equations, p represents population and $T = t/r$ is a ratio of t most fitted individuals selected from population of size r for reproduction.

Sample bifurcation diagrams are depicted in Figs. 3.92 - 3.95. Ideas about chaos in simple genetic algorithm are explained in detail in [32]. In this chapter, it has been proven that chaos in heuristic algorithms can be observed. This observation is certainly not valid only for simple genetic algorithms.

$$F_T(p) = \begin{cases} 1 & \text{if } T < p \\ \frac{p}{T} & \text{if } T > p \end{cases} \quad (3.38)$$

$$U_{a,b}(p) = p - \frac{b}{2} |2p - 1|^a (2p - 1) \quad (3.39)$$

3.5.10 Astronomy – The Three-Body Problem

Quite a number of systems are encountered in astrophysics exhibiting chaotic behavior. As a typical example, let us discuss the three-body problem. This is a celestial mechanics problem describing the motion of three (or more) bodies affecting one another by gravitational forces. Mathematically, the three-body problem is formulated by a system of equations of motion, see (3.40).

$$m_j \ddot{q}_j = \gamma \sum_{k \neq j}^n \frac{m_k m_j (q_j - q_k)}{|q_j - q_k|^3}, \quad j = 1, \dots, n \quad (3.40)$$

In this system of equations, m is the mass of the mutually affecting bodies and q is a vectorial function of time defining the positions of the bodies. The problem of n bodies involves $6n$ variables (because each body has 3 position components and 3 velocity components). The motion of a system of n bodies is practically analytically unsolvable starting from $n = 3$, and simulations of the behavior are performed numerically on computers. This problem attracted interest of such mathematicians as Euler (1767, discovery of collinear periodic trajectories), Lagrange (1772, central configuration of a system of n bodies), Charles-Eugene Delaunay (1860-1867, a study 900 pages volume dealing with the Earth-Moon-Sun system).

A simplified version of the three-body problem, called the restricted three-body problem, has been formulated in this context. In this simplification, the mass of one of the bodies is disregarded or the trajectories of the bodies are reduced to some shapes such as circular or elliptical. Fig. 3.96 - 3.99 shows the behavior of three bodies for different initial conditions. Chaotic behavior, or more precisely chaotic orbits of the three bodies are clearly seen.

The n -body problem (or more precisely its restricted version) can also be simulated by means of a relatively simple device called a mad pendulum. This pendulum consists of N magnets located in the apexes of an N -angle, above which hangs a steel ball on a thin string (see Fig. 3.100). The mathematical model describing the behavior of the pendulum is given by (3.41).

$$\begin{aligned}
 -\sum_{i=1}^6 \frac{X_i - x(t)}{\sqrt{d^2(X_i - x(t))^2 + (Y_i - y(t))^2}} + sc * x(t) + R * \dot{x}(t) + \ddot{x}(t) &= 0 \\
 -\sum_{i=1}^6 \frac{Y_i - y(t)}{\sqrt{d^2(X_i - x(t))^2 + (Y_i - y(t))^2}} + sc * y(t) + R * \dot{y}(t) + \ddot{y}(t) &= 0
 \end{aligned} \tag{3.41}$$

Each magnet attracts in some way the ball suspended from the starting position, and a chaotic trajectory results. For example, Fig. 3.100 - 3.101 shows two trajectories which are entirely different although the starting conditions only differ by one-hundredth in the velocity.

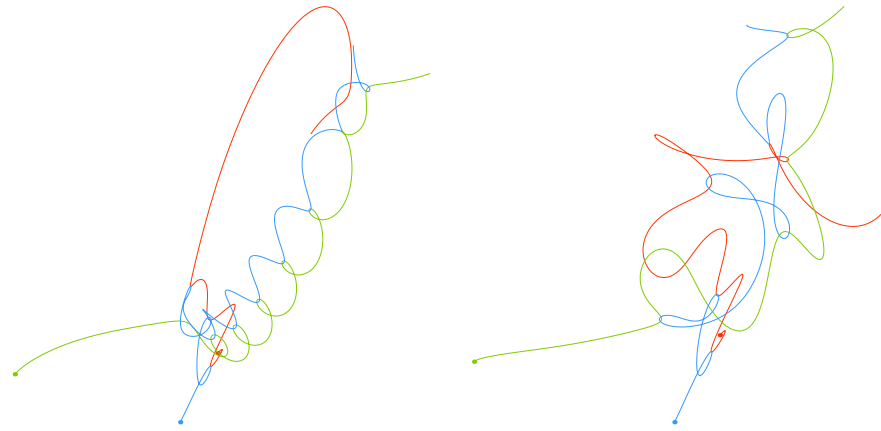


Fig. 3.96 Three body problem - random initial conditions

Fig. 3.97 Three body problem - different initial conditions



Fig. 3.98 Three body problem - different initial conditions

Fig. 3.99 Three body problem - different initial conditions

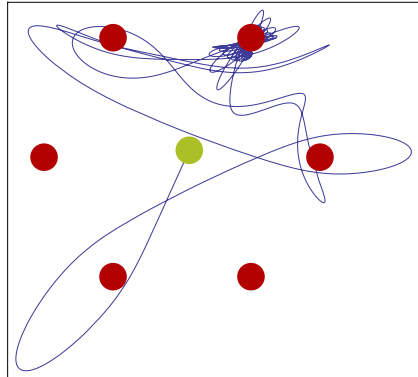


Fig. 3.100 Trajectories of a mad pendulum for $v_{x,y} = -1.05, -2.31\dots$

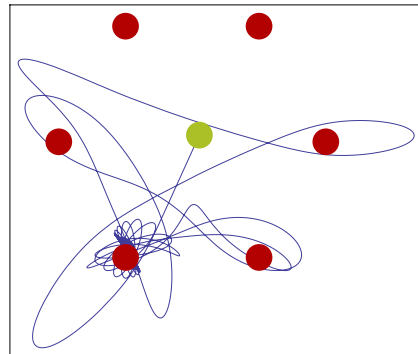


Fig. 3.101 ... and another trajectories for $v_{x,y} = -1.05, -2.3$.

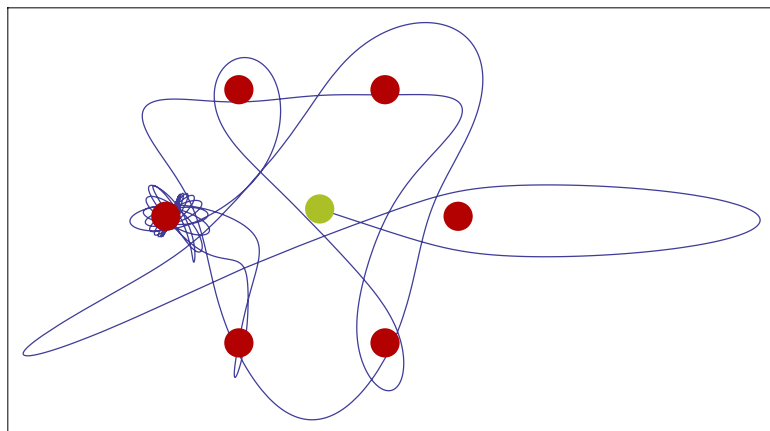


Fig. 3.102 Another trajectory for $v_{x,y} = 3, -1$

It is clear from the pictures and from the physical nature of the problem that the chaotic mode can only be observed during a certain time interval. Due to energy dissipation the pendulum will eventually stay in the resting position at one of the magnets or in the origin of the N -angle. Fig. 3.103 shows the development of the x -component of the pendulum motion. Chaotic behavior can be observed during the first 20 seconds of development. Subsequently, chaos vanishes due to energy dissipation, quasi-periodic oscillation follows, and ultimately the pendulum remains at rest.

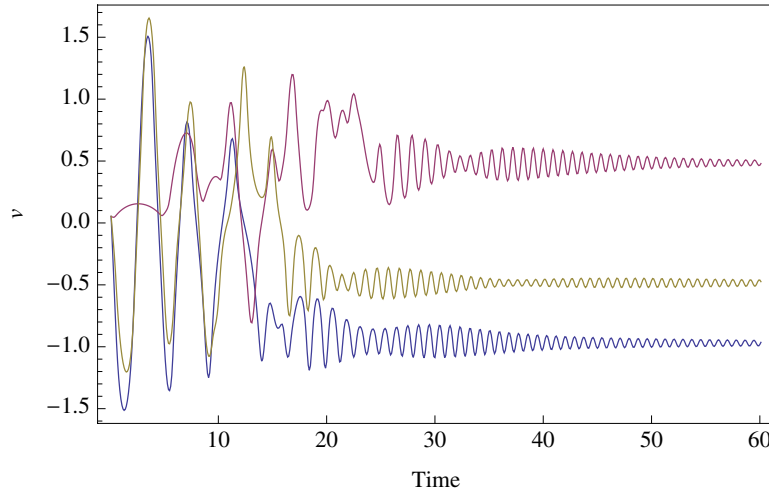


Fig. 3.103 Time development of the behavior of the pendulum for different starting values of $v_{x,y}$

3.6 Conclusion

This chapter presents a very simple introduction to deterministic chaos theory. Main and well known icons of chaos, like Lyapunov exponent, Feigenbaum's constant, U-sequence, self-similarity etc has been introduced. The way how deterministic behavior can be changed into a chaotic one is also discussed like intermittence, period doubling, crises as well as chaotic transients. At the end of this chapter, selected examples from mechanics, astrophysics, computer sciences, electronics amongst others are described. Main attention has been paid to demonstration of deterministic chaos behavior. For more detailed explanation and description of deterministic chaos it is recommended to study literature in the references.

Acknowledgements. This work was supported by grant No. MSM7088352101 of the Ministry of Education of the Czech Republic and by grants of the Grant Agency of the Czech Republic GACR 102/09/1680 and 102/08/0186.

References

1. Abarbanel, H.: Analysis of observed chaotic data. Springer, New York (1996)
2. Abarbanel, H., Brown, R., Kennel, M.: Variation of Lyapunov exponents on a strange attractor. *J. Nonlinear Sci.* 1, 175 (1991)
3. Alligood, K., Sauer, T., Yorke, J.: Chaos - an introduction to dynamical systems. Springer, New York (1997)
4. Arnold, V.: The Theory of Singularities and Its Applications, Accademia Nazionale Dei Lincei, Pisa, Italy (1991)

5. Baker, G., Gollub, J.: *Chaotic dynamics: an introduction*. Cambridge University Press, Cambridge (1996)
6. Barnsley, M.: *Fractals Everywhere*. Academic Press Professional, London (1993)
7. Bose, N., Liang, P.: *Neural Network Fundamentals with Graphs, Algorithms, and Applications*. McGraw-Hill Series in Electrical and Computer Engineering (1996)
8. Constantin, P., Foias, C.: Global Lyapunov exponents, Kaplan-Yorke formulas and the dimension of attractors for 2D Navier-Stokes equations. *Commun. Pure Appl. Math.* 38, 1 (1985)
9. Cvitanovic, P.: *Universality in Chaos*. Taylor and Francis, Abington (1989)
10. Diks, C.: Nonlinear time series analysis, Methods and applications. World Scientific, Singapore (1999)
11. Drazin, P., Kind, G.(eds.): Interpretation of time series from nonlinear Systems. Special issue of *Physica D*, 58 (1992)
12. Galka, A.: Topics in nonlinear time series analysis with implications for EEG analysis. World Scientific, Singapore (2000)
13. Gilmore, R.: *Catastrophe Theory for Scientists and Engineers*. John Wiley and Sons, Chichester (1993)
14. Haken, H.: *Synergetics: Introduction and Advanced Topics*. Springer, Heidelberg (2004)
15. Kaplan, J., Yorke, J.: Chaotic behavior of multidimensional difference equations. In: Walter, H., Peitgen, H. (eds.) *Functional differential equations and approximation of fixed points*. Lect. Notes Math., vol. 730, p. 204. Springer, Berlin (1979)
16. Hilborn, R.: *Chaos and Nonlinear Dynamics*. Oxford University Press, Oxford (1994)
17. Kantz, H., Schreiber, T.: *Nonlinear time series analysis*. Cambridge University Press, Cambridge (1997)
18. Ledrappier, F., Young, L.: The metric entropy of diffeomorphisms, Parts I and II. *Ann. Math.* 122, 509 (1985)
19. Packard, N., Crutchfield, J., Farmer, D., Shaw, R.: Geometry from a time series. *Phys. Rev. Lett.* 45, 712 (1980)
20. Pesin, Y.: Characteristic Lyapunov exponents and smooth ergodic theory. *Russ. Math. Surv.* 32, 55 (1977)
21. Poston, T., Stewart, I.: *Catastrophe Theory and its Applications*, Pitman, pp. 842–844. IEEE Press, New York (1977)
22. Rössler, O.: An equation for hyperchaos. *Phys. Lett. A* 71, 155 (1979)
23. Ruelle, D.: *Thermodynamics Formalism*. Addison-Wesley, Reading (1978)
24. Schuster, H.: *Handbook of Chaos Control*. Wiley-VCH, New York (1999)
25. Sprott, J.: *Chaos and Time-Series Analysis*. Oxford University Press, Oxford (2003)
26. Takens, F.: Detecting strange attractors in turbulence. *Lecture Notes in Math.*, vol. 898 (1981)
27. Vose, M.: *The Simple Genetic Algorithm: Foundations and Theory*. MIT Press, Cambridge (1999)
28. Vose, M., Liepins, G.: Punctuated equilibria in genetic search. *Complex Systems* 5, 31–44 (1991)
29. Vose, M., Wright, A.: Simple genetic algorithms with linear fitness. *Evol. Comput.* 4(2), 347–368 (1994)
30. Wolff, R.: Local Lyapunov exponents: Looking closely at chaos. *J. R. Statist. Soc. B* 54, 301 (1992)
31. Wolfram, S.: *A New Kind of Science*, Wolfram Media (2002)
32. Wright, A., Agapie, A.: Cyclic and Chaotic Behavior in Genetic Algorithms. In: Proc. of Genetic and Evolutionary Computation Conference (GECCO), San Francisco, July 7-11 (2001)
33. Wyk, M.: *Chaos in Electronics*. Springer, Heidelberg (1997)

